

**Aus dem Institut für Medizinische Mikrobiologie  
und Hygiene der Universität Tübingen,  
Ärztlicher Direktor: Professor Dr. I. B. Autenrieth**

**Mukoviszidose ist eine Autoimmunkrankheit**

**Inaugural-Dissertation  
zur Erlangung des Doktorgrades der Zahnheilkunde**

**der Medizinischen Fakultät  
der Eberhard Karls Universität zu Tübingen**

**Vorgelegt von  
Cheyla Conceição de Oliveira-Munding  
aus Angical, Brasilien**

**2006**

<b>Dekan:</b>	<b>Professor Dr. I. B. Autenrieth</b>
<b>1. Berichterstatter:</b>	<b>Professor Dr. G. Döring</b>
<b>2. Berichterstatter:</b>	<b>Professor Dr. M. Stern</b>

## CONTENTS

---

	<b>Page</b>
<b>1. INTRODUCTION</b>	<b>5</b>
1.1. <b>Epidemiology of cystic fibrosis</b>	<b>5</b>
1.2. <b>Structure, function and localization of CFTR</b>	<b>5</b>
1.3. <b>The relation between CFTR and lung disease</b>	<b>7</b>
1.4. <b>Natural killer T cells</b>	<b>10</b>
1.5. <b>Aim of the study</b>	<b>13</b>
<b>2. MATERIALS AND METHODS</b>	<b>14</b>
2.1. <b>Chemicals, reagents und buffer</b>	<b>14</b>
2.2. <b>Media</b>	<b>14</b>
2.3. <b>Mouse strains</b>	<b>15</b>
2.4. <b>Antibodies, used for cell characterization in the study</b>	<b>17</b>
2.5. <b>Immunofluorescence staining of murine tissues</b>	<b>17</b>
2.6. <b>PAS staining of murine lung tissue</b>	<b>18</b>
2.7. <b>Immunohistochemistry staining of murine tissues</b>	<b>18</b>
2.8. <b>Statistics</b>	<b>19</b>
<b>3. RESULTS</b>	<b>20</b>
3.1. <b>Accumulation of NKT cells in submucosal glands of CFTR<sup>-/-</sup> mice</b>	<b>20</b>
3.2. <b>NKT cell accumulation progresses with the age of CFTR<sup>-/-</sup> mice</b>	<b>22</b>
3.3. <b>Accumulation of macrophages and neutrophils in CFTR<sup>-/-</sup> mice</b>	<b>26</b>
3.4. <b>Acumulation of ceramide in mucosa and submucosal</b>	

	<b>tissue of CFTR<sup>-/-</sup> mice</b>	<b>30</b>
<b>3.5.</b>	<b>Amitriptyline reduces ceramide expression and NKT cells in CFTR<sup>-/-</sup> mice</b>	<b>31</b>
<b>3.6.</b>	<b>Accumulation of NKT cells in intestinal tissues of CFTR<sup>-/-</sup> mice</b>	<b>33</b>
<b>3.7.</b>	<b>Accumulation of other immunocompetent cells in respiratory submucosal glands of CFTR<sup>-/-</sup> mice</b>	<b>36</b>
<b>3.8.</b>	<b>Lymphocyte aggregates are present around respiratory submucosal glands of CFTR<sup>-/-</sup> mice</b>	<b>38</b>
<b>4.</b>	<b>DISCUSSION</b>	<b>40</b>
<b>5.</b>	<b>REFERENCES</b>	<b>46</b>
<b>6.</b>	<b>ABSTRACT</b>	<b>52</b>
<b>7.</b>	<b>Curriculum vitae</b>	<b>53</b>
<b>8.</b>	<b>Acknowledgements</b>	<b>55</b>

---

## **1. INTRODUCTION**

### **1.1. Epidemiology of Cystic Fibrosis**

Cystic fibrosis (CF) is the most common fatal inherited disease in the Caucasian population, affecting about 1:2,500 children, with a carrier frequency of 1:25 [1]. CF is caused by mutations in a 230 kB gene on chromosome 7 encoding a 1480 amino acid polypeptide named cystic fibrosis transmembrane conductance regulator (CFTR) [2-4]. The disease is diagnosed on clinical symptoms including persistent cough and diarrhea caused by pancreatic insufficiency. The single most useful diagnostic procedure is the sweat test with chloride concentrations  $> 60\text{mmol/L}$  in typical cases of CF. Generally, the diagnosis is confirmed by genotyping of the most common CFTR mutations which vary between different geographic regions. Over 1,200 mutations and sequence variants have been described to date and reported to the Cystic Fibrosis Genetic Analysis Consortium [5]. Most of these mutations are rare and only 4 mutations occur in a frequency of more than 1%. CFTR mutations are grouped into five classes: defective synthesis (I), defective processing (II), defective regulation (III), defective conductance (IV) partially defective production or processing (V) [6]. Class I-III mutations are more common and associated with pancreatic insufficiency. Patients with the rarer class IV-V mutations often are pancreatic sufficient. The most common mutation worldwide is a class II mutation caused by a deletion of phenylalanine in position 508 (F508del) of the CFTR protein leading to misfolding. Of 43,849 CF chromosomes tested, 66% are F508del. Linking mutations to the severity of lung disease has been unsuccessful and patients who are homozygous for the F508del mutation exhibit a wide spectrum in the rate of development and severity of lung disease, suggesting the presence of modifier genes. Prognosis of CF has improved dramatically in some but not all countries as a result of better care and therapy and most children now reach adult life.

### **1.2. Structure, Function and Localization of CFTR**

CFTR functions as a chloride channel in apical membranes [7, 8]. The primary structure of CFTR indicated that it belongs to a family of transmembrane proteins called ATP-binding cassette (ABC) transporters [8, 9]. ABC transporters (or traffic ATPases) form a large family of proteins responsible for the translocation of a variety of compounds across



functional abnormalities have been shown in the heart or the placenta, both sites of CFTR expression, and the electrolytes of ocular humour, breast milk and seminal fluid are not significantly altered in CF.

CF leads to pathologic changes in organs that express CFTR; therefore secretory cells, sinuses, lungs, pancreas, liver and reproductive tract are involved. The most dramatic changes are observed in CF airways where the basic defect causes mucus retention, chronic bacterial infection and inflammation. Lung infections with *Pseudomonas aeruginosa* constitute a predominant disease phenotype in CF patients. Chronic bacterial lung infections are responsible for most of the morbidity and mortality in CF [17]. Infections with *Staphylococcus aureus* and *Haemophilus influenzae* are also frequent.

### **1.3. The Relation between CFTR and Lung Disease**

Several hypotheses have been offered to explain the failure of mucosal defense in the CF lung. One of these hypothesizes that inflammation precedes infection. Autopsy specimens from neonates with CF who have not yet developed lung disease show luminal dilation in submucosal glands [18]. This may indicate mucus accumulation. Indeed elevated viscosity has been detected in CF submucosal glands, which was interpreted to promoting bacterial colonization and airway disease in CF patients due to impaired mucociliary clearance and antimicrobial defense mechanisms [19]. Staining of immune cells revealed significant differences between CF and non-CF fetal airways concerning the numbers of mast cells and macrophages [20]. Already in the first months of life inflammatory infiltrates in bronchi and mucopurulent plugging of airways can be detected histologically [21]. Both the number of neutrophils and levels of a neutrophil attracting IL-8, were increased in bronchoalveolar lavage (BAL) of CF infants as young as 4 weeks who had negative cultures for common bacterial CF-related pathogens [22, 23]. How is neutrophil activation related to infection? Lysosomal enzyme release and enhanced production of reactive oxygen species may facilitate bacterial infection. The release of host proteases during acute and chronic inflammation may damage epithelial cells thereby facilitating *P. aeruginosa* adhesion *in vitro* and *in vivo* [23, 24].

The notion that inflammation precedes bacterial lung infection is also supported by cell culture studies, revealing increased toll-like receptor expression [25], increased NFkB acti

vation [26, 27] and increased baseline IL 8 production [27] in CF cells versus controls. Most of the uncertainties in this context derive from the fact that it is difficult generally start very early after birth in these patients. Only one study was reported which revealed an increased immune cell infiltration into the CF mucosa [28].

Therefore, CF mouse models have been developed [29-31]. The expression of human CFTR in CFTR<sup>-/-</sup> mice under the control of the rat intestinal fatty acid-binding (FAB) protein gene promoter [31], resulted in prolonged survival of the animals and allowed to study CF-related lung disease more closely. Support of the hypothesis that inflammation precedes infection stems from a study in germ-free raised CF mice which showed signs of inflammation [32] and sterile fetal CF airways, transplanted into severe combined immunodeficiency mice [33, 34]. An increased IL-8 production and increased neutrophil infiltration was observed (**Fig. 2**). Furthermore, long-lived C578L/6J CFTR<sup>-/-</sup> mice develop CF-like disease [35, 36] and are more susceptible to bacterial infection [37, 38]. CF like morphology such as defective mucociliary transport and neutrophilic inflammation in the absence of infection are also seen in mice overexpressing the beta subunit of the epithelial sodium channel [39]. However, others groups have not confirmed some of these findings. Thus, in newly diagnosed CF infants under the age of six months [40], and in a group of CF patients up to 48 months of age [41], inflammatory BAL markers correlated with the presence of infection and decreased when pathogens were eradicated.



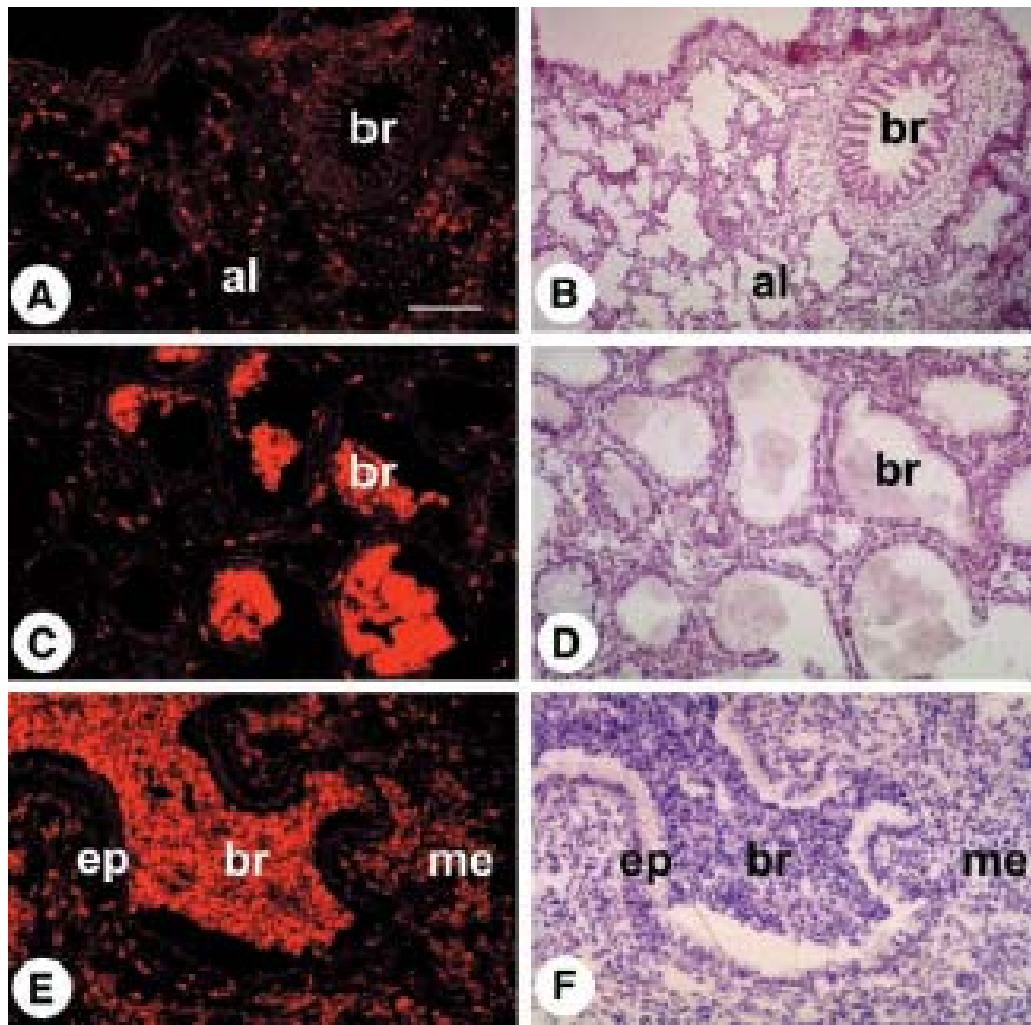


**Fig. 2. Murine leukocytes infiltrate into the lumen of long-term CF grafts.** *A*: mature non-CF graft (gestational age, 16 wk; engraftment time, 15 wk) showing Ly5<sup>+</sup> murine leukocytes in the mesenchyme but not in the lumen of bronchiolar (br) and alveolar (al) areas. *B*: bright-field view of *A*. *C*: mature CF graft (16 + 15 wk) showing Mac1<sup>+</sup> murine leukocytes in the lumen of bronchioles (br). Note that some, but not all, luminal areas are infiltrated with murine leukocytes. *D*: bright-field view of *C*. *E*: detail of mature CF graft (12 + 28 wk) showing Gr1<sup>+</sup> mouse neutrophils packed in the mesenchyme (m), epithelium (e), and bronchiolar lumen (br). *F*: bright-field view of *E*. Scale bars: 200  $\mu$ m in *A* and *B*, 100  $\mu$ m in *C* and *D*, and 50  $\mu$ m in *E* and *F* (from [34]).

Several other hypotheses have been offered to explain the failure of mucosal defense and the high prevalence of *P. aeruginosa* in the CF lung. It has been proposed that *P. aeruginosa* binds to CF airway epithelial cell membranes in higher density than to respective cells

from normal individuals due to an increased *P. aeruginosa* asialo-GM1 receptor density [42, 43]. The higher bacterial number would then lead to infection in CF airways. Other studies, however, reveal that both *P. aeruginosa* and *S. aureus* are located in the mucus layer on respiratory epithelial cells rather than directly on cell membranes and that no difference in location and number of adhering bacteria is visible regardless whether normal or CF primary respiratory cells are used, or infected CF lung tissue is investigated for *P. aeruginosa* or *S. aureus* adhesion [44, 45]. Alternatively, also wild type CFTR (but not mutated CFTR) has been shown to be a receptor for *P. aeruginosa* which mediates bacterial cell internalization and *P. aeruginosa* killing. In CF airways, therefore, *P. aeruginosa* would not be eradicated intracellularly and could multiply and cause infection [46]. Additionally, based on the assumption of an increased sodium chloride concentration due to a defective CFTR channel on the luminal side of the respiratory epithelium, it has furthermore been suggested that salt sensitive cationic antimicrobial peptides (defensins) are inactivated in the airway surface liquid (ASL) of CF patients which would lead to bacterial multiplication and subsequent infection [47]. However, not all defensins are salt-sensitive and it has been difficult to prove that the ASL in CF is indeed hypertonic. In contrast, most in vivo data reveal that the ASL from normal and CF individuals is isotonic [48].

The hypothesis of defective mucociliary clearance in CF airways is based on the assumption that chloride secretion into the airway surface liquid is inhibited by mutated CFTR, leading to sodium hyperabsorption, leaving the luminal site hypotonic. To establish isotonic conditions, increased water absorption occurs from the luminal site which leads to a volume/height depletion of the airway surface liquid, resulting in mucus stasis [48, 49]. The higher viscoelasticity of the CF mucus layer and submucosal gland secretions may also influence innate immunity functions within these areas [50, 51].

#### **1.4. Natural killer T cells**

Given the evidence that inflammation precedes infection in CF, the possibility arises that natural killer T (NKT) cells may recognize the abnormal cells in organs which express altered CFTR or lack CFTR. NKT cells are a specialized subset of T lymphocytes which express a very limited T cell receptor (TCR) repertoire, consisting of an invariant TCR $\alpha$  chain (murine: V $\alpha$ 14J $\alpha$ 18) and a restricted, yet not invariant TCR $\beta$  (V $\beta$ 11) repertoire [52-

54]. Most NKT cells are characterized by the co-expression of the NKT cell surface marker, NK1.1, and an antibody directed against the T cell receptor.

NKT cells react to several glycolipide antigens presented by the MHC class I-like molecule, CD1d on antigen presenting cells [55-58]. One of these, isoglobotrihexosylceramide (iGb3) is an endogenous lysosomal glycosphingolipid, derived from lysosomal degradation of iGb4 via  $\beta$ -hexosaminidase [56] (**Fig. 3**).  $\beta$ -hexosaminidase removes the terminal Gal-Nac of iGb4 in the lysosome to produce iGb3. The  $\alpha$ -galactosidase A transforms subsequently iGb3 into lactosylceramide.

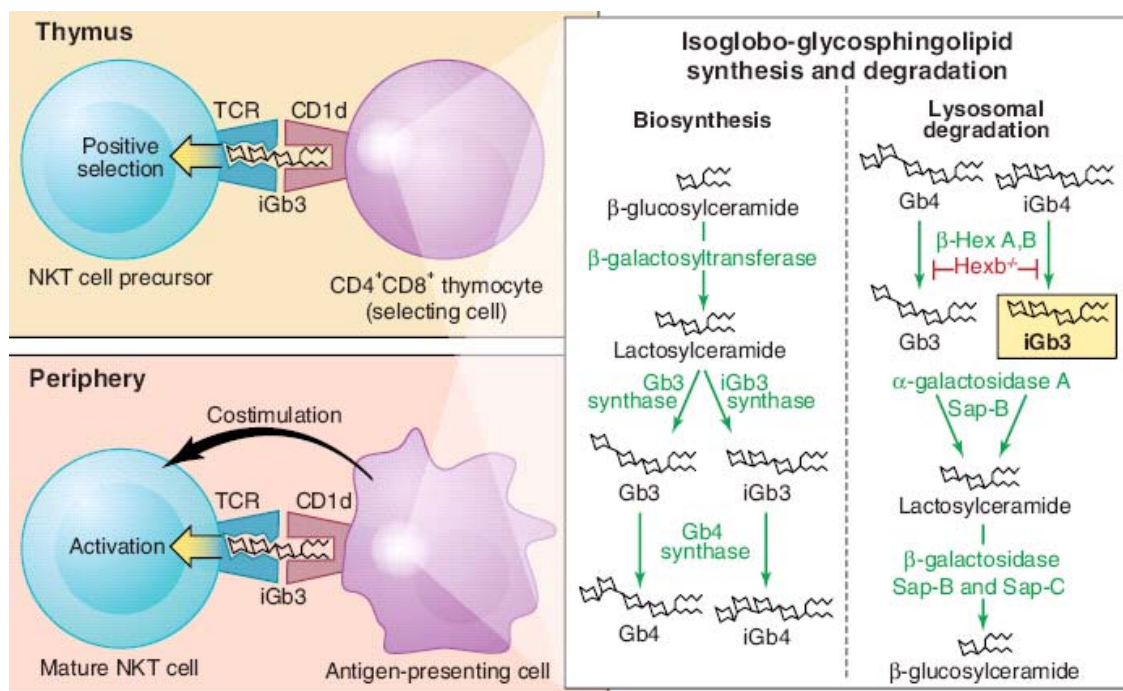


**Fig.3. An antigen for NKT cells.** The TCR of NKT cells recognizes the glycosphingolipid iGb3 presented in the context of CD1d. Recognition of iGb3 occurs during NKT cell selection in the thymus (**top**) and activation in the periphery (**bottom**). Loading of iGb3 into CD1d first requires biosynthesis of the isoglyco-series glycosphingolipids and the subsequent degradation of these molecules in lysosomes by the enzymes  $\beta$ -hexosaminidase A and B (**box**) (from ref [59]).

Natural killer cells release Th1 cytokine such as  $\gamma$ -IFN and TNF $\alpha$ , but also Th2 cytokines such as IL-4, IL-10 and IL-13. The production of TH1 and TH2 cytokines from NKT cells are thought to be important for suppression of autoimmunity, promotion of tumor im

munity and suppression of allergy and inflammation [60, 61] (Fig. 4).

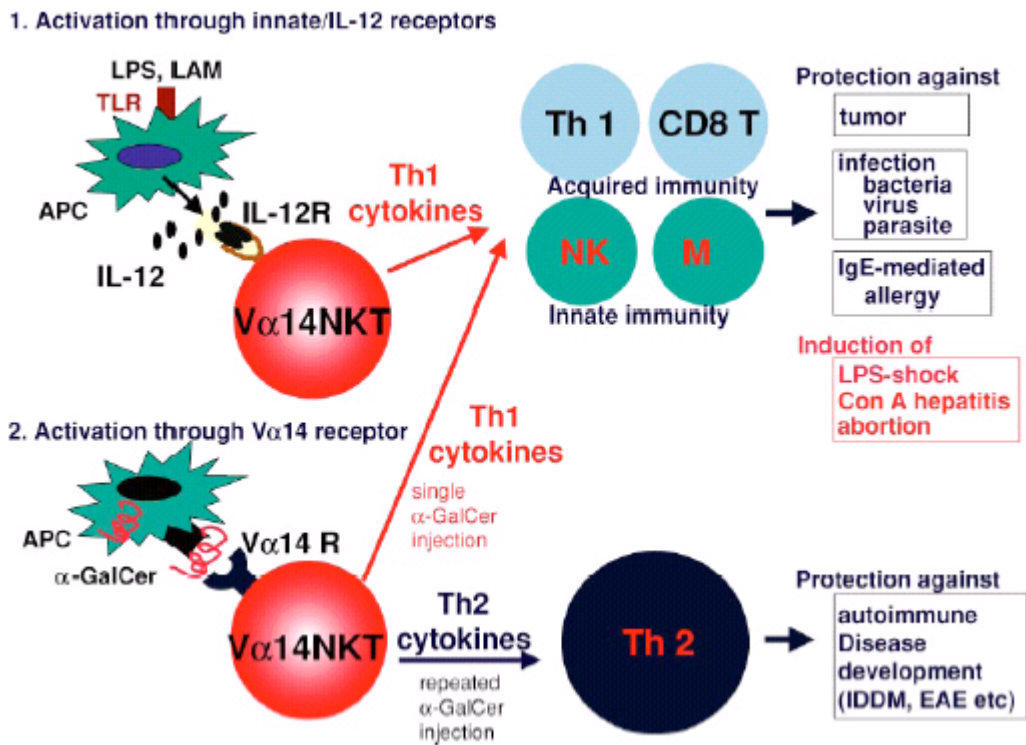


**Fig. 4.** Schematic diagram of  $V\alpha 14$  NKT cell activation and their interactions. Two types of activation pathways, through innate immune system/IL-12 receptor and through specific recognition of the  $\alpha$ -GalCer ligand, are represented. Each activation pathway displays different functional activities of  $V\alpha 14$  NKT cells. TLR, Toll-like receptor; APC, antigen presenting cells; LPS, lipopolysaccharide; LAM, lipoarabinomannane; M, macrophage (from [61]).

### **1. 5. Aim of the study**

Based on the notion that inflammation may precede infection in CF, the aim of the study was to investigate whether the CF defect would be recognized by cells of the innate immune system. Specifically, uninfected CF mouse strains and the respective wild type strains of different ages should be used to locate and quantify NKT cells, macrophages and neutrophils and other immunocompetent cells in organs which express CFTR. A second aim of the present study was to test the hypothesis that ceramide accumulates in lung of CFTR<sup>-/-</sup> mice.

## 2. MATERIALS AND METHODS

### 2.1 Chemicals, reagents und buffer

Ethanol	(Merk, Darmstadt)
Xylene	(Merk, Darmstadt)
Tween 20	(Sigma, Deisenhofen)
Solvent resistant Pen	(DAKO, Hamburg)
Cover slip	(R. Langenbrinck, Emmendingen)
Hämatoxylin	(Sigma, Deisenhofen)
Formaldehyde	(Sigma, Deisenhofen)
Hydrogen peroxide 3%	(Sigma, Steinheim, Germany)
Chem Mate-Target Retrieval Solution x10	(DAKO Hamburg)
Aceton	(Merk, Darmstadt)
Proteinase K	(DAKO Hamburg)
AEC Peroxidase Substrate Kit	(Vector Laboratories)
Vector Nova Red Substrate Kit	(Vector Laboratories)
Fluorescent Mounting Medium	(DAKO Hamburg)
Faramount, Aqueous Mounting Medium	(DAKO Hamburg)
Fisher Superfrost slide	(R. Langenbrinck, Emmendingen)
BCIP/NBT Substrate	(Vector Laboratories)

### 2.2 Media

#### 2.2.1 Phosphate-Buffered Saline (PBS) x 20

85, 00 g NaCL

14, 23 g Na<sub>2</sub>HPO<sub>4</sub> x12 H<sub>2</sub>O

1, 35 g KH<sub>2</sub>PO<sub>4</sub>

1, 00 g NaN<sub>3</sub>

Mix in 500 ml distilled water.

### **2.2.2 PBS-Tween**

Dilute PBS x 20 1:20 in 1 l distilled water and mix with 2 ml Tween 20.

### **2.2.3 Formaldehyde 4%**

Dilute formaldehyde 37% 1:9 with distilled water and store at 4°C.

### **2.2.4 Triton X 100/Tween**

Dilute Triton X 100 1:200 in PBS-Tween.

### **2.2.5 Chem Mate (Target Retrieval Solution)**

Mix 180 ml distilled water and 20 ml Chem Mate solution.

**2.3 Mouse strains.** The following mouse strains with C57Bl/6NCrl background were used. (Table 1). Anna M. van Heeckeren, Case Western Reserve University, Cleveland, USA provided CF mice with a S489X mutation in CFTR. Hugo de Jonge, Erasmus University, Rotterdam, The Netherlands, provided CF mice with a F508 deletion in CFTR. Uta Griesenbach, Imperial College London, England, provided gut-corrected FABp CF mice on UNC-Null background, originally made by Jeff Whitsett. The same CF strain, treated with the ASMase blocker amitryptilin was provided by Erich Gulbins, Institut für Molekularbiologie, Universitätsklinikum Essen. Erich Gulbins also provided a CFTR<sup>-/-</sup>ASM<sup>-/-</sup> double mutant mouse strain.

**Table1. Age, number, genotype and origin of mice, used in the study.**

<b>Age</b>	<b>Sample #</b>	<b>Section #</b>	<b>Mause #</b>	<b>CFTR genotype ++</b>	<b>CFTR genotype -/-</b>	<b>CFTR -/- ASM -/-</b>	<b>A<sup>1</sup></b>
<b>10</b>	<b>4</b>	<b>48</b>	<b>4</b>	<b>4<sup>2</sup></b>	<b>0</b>		<b>0</b>
<b>12</b>	<b>18</b>	<b>216</b>	<b>18</b>	<b>9<sup>3</sup></b>	<b>9<sup>3</sup></b>		<b>0</b>
<b>14</b>	<b>4</b>	<b>48</b>	<b>4<sup>2</sup></b>	<b>4<sup>2</sup></b>	<b>0</b>		<b>0</b>
<b>18</b>	<b>4</b>	<b>48</b>	<b>4</b>	<b>0</b>	<b>4<sup>2</sup></b>		<b>0</b>
<b>22</b>	<b>3</b>	<b>36</b>	<b>3</b>	<b>0</b>	<b>0</b>	<b>3<sup>4</sup></b>	<b>0</b>
<b>24</b>	<b>4</b>	<b>36</b>	<b>4</b>	<b>4<sup>2</sup></b>	<b>0</b>	<b>0</b>	<b>0</b>
<b>28</b>	<b>24</b>	<b>240</b>	<b>24</b>	<b>2<sup>4</sup></b>	<b>14<sup>2</sup></b>	<b>0</b>	<b>8<sup>4</sup></b>
<b>30</b>	<b>10</b>	<b>120</b>	<b>10</b>	<b>0</b>	<b>25<sup>2</sup></b>	<b>0</b>	<b>5<sup>4</sup></b>
<b>34</b>	<b>12</b>	<b>72</b>	<b>2</b>	<b>1<sup>5</sup></b>	<b>1<sup>5</sup></b>	<b>0</b>	<b>0</b>
<b>52</b>	<b>18</b>	<b>216</b>	<b>18</b>	<b>6<sup>2</sup></b>	<b>6<sup>2</sup></b>	<b>0</b>	<b>6<sup>4</sup></b>

1: CFTR -/-, Amitriptyline; 2: from Uta Griesenbach; 3: from Anna M. van Heeckeren; 4: from Erich Gulbins; two CFTR+/+ mice, 28 week old were infected with *P. aeruginosa*; 5: from Hugo de Jonge.



## 2.4 Antibodies, used for cell characterization in the study.

---

Monoclonal antibody to ceramide	(Alexis)
Monoclonal antibody to mouse CD68	(Acris)
Monoclonal antibody to mouse neutrophils	(Acris)
Monoclonal antibody to mouse NKG2D	(R&D System)
Monoclonal antibody to mouse CD3e	(R&D System)
Monoclonal antibody to mouse NK1.1	(eBioscience)
Monoclonal antibody to mouse CD4	(eBioscience)
Monoclonal antibody to mouse CD25	(eBioscience)
Cy2 conjugated Goat antibody to Rabbit IgG (H+L) (Dianova)*	
Cy2 conjugated Goat antibody to Syrian Hamster IgG (H+L)	(Dianova)*
Cy2 conjugated Goat antibody to Rat IgG (H+L)	(Dianova)*
Cy2 conjugated Goat antibody to mouse IgG (H+L)	(Dianova)*
Cy3 conjugated Goat antibody to Rat IgG (H+L)	(Dianova)*
Cy3 conjugated Goat antibody to mouse IgG (H+L)	(Dianova)*
Cy3 conjugated Goat antibody to Rabbit IgG (H+L)	(Dianova)*

---

\*: Second antibody

**2.5 Immunofluorescence staining of murine tissues.** Staining of murine tissues was done by indirect immunofluorescence using different antibodies (table) as described previously by Ulrich et al. [44].

1. Prepare cryostat thin sections (5–10  $\mu\text{m}$ ) (Kryostat 2800 Frigocut E; Reichert-Jung, Heidelberg, Germany) from shock-frozen lung tissue material.
2. Fix thin sections on cover slips with acetone for 5 min.
3. Wash cover slips with PBS-Tween for 15 min.
4. Preincubate cover slips with normal goat serum, 1:10 diluted in PBS-Tween for 30 min.

5. Wash 3X with PBS-Tween for 5 min
6. Incubate with first antibody in respective dilutions in Triton 0, 5% for 1 h at room temperature or overnight at 4° C
7. Wash 3X with PBS-Tween for 5 min
8. Incubate with second antibody Cy2-labeled in respective dilutions in Triton 0, 5% for 1 h at room temperature
9. Wash 3X with PBS-Tween for 5 min
10. Incubate with DAPI 1:500 in PBS-Tween for 5 min at room temperature
11. Wash 3X with PBS-Tween for 5 min
12. Embedd with Fluorescent Mouting Medium and cover slip (24 x 60 mm)
13. Store in refrigerator at 4°C before microscopic examination

## **2.6 PAS staining of murine lung tissue.**

1. Wash tissue sections 1– 15 min in PBS-Tween
2. Incubate sections with periodic acid for 5 min.
3. Wash with distilled water
4. Incubate sections with Schiff's reagent for 15 min.
5. Wash with warm water (20-25°C)
6. Stain with Hematoxylin for 1 min.
7. Wash with water for 5 min
8. Embedd with DAKO Faramount Aqueous Mouting Medium and cover slips (24 x 60 mm).
9. Store in refrigerator at 4°C overnight before microscopical examination.

**2.7 Immunohistochemistry staining of murine tissues.** Staining of murine tissues was done by indirect immunohistochemistry using different antibodies (table) as described previously by Ulrich et al. [44].

1. Prepare cryostat thin sections (5–10 µm), (Kryostat 2800 Frigocut E; Reichert-Jung, Heidelberg, Germany) from shock-frozen lung tissue material.

2. Fix thin sections on cover slips with acetone for 5 min.
3. Wash cover slips with PBS-Tween for 15 min.
4. Preincubate cover slips with Endogenous Alkaline Phosphatase Inhibitor 15 min.
5. Wash 3X with PBS-Tween for 5 min.
6. Preincubate cover slips with normal goat serum, 1:10 diluted in PBS-Tween for 30 min.
7. Wash 3X with PBS-Tween for 5 min .
8. Incubate with first antibody in respective dilutions in Triton 0.5% for 1 h at room temperature or overnight at 4° C
9. Wash 3X with PBS-Tween for 5 min.
10. Incubate with second antibody APAAP-labeled in respective dilutions in Triton 0.5 % for 1 h at room temperature.
11. Wash 3X with PBS-Tween for 5 min.
12. Incubate with BCIP /NBT Substrate 20 min at room temperature.
13. Wash 3X with PBS-Tween for 5 min.
14. Incubate with Hämatoxylin for 1min.
15. Wash 3X with PBS-Tween for 5 min.
16. Embedd with Aquous Mouting Medium and cover slip (24 x 60 mm).
17. Store in refrigerator at 4°C before microscopic examination.

**2.8. Statistics.** To calculate statistically the numbers of immune cells in mouse tissues the Student's t-test was applie, using Microsoft Excel 0.5.

### 3. RESULTS

#### 3.1 Accumulation of NKT cells in submucosal glands of CFTR<sup>-/-</sup> mice.

Based on the hypothesis, that cells expressing mutated CFTR (or cells which do not express CFTR at all) are recognized by the innate immune system, lung tissue of CFTR<sup>-/-</sup> mice was stained for NKT cells using NK1.1 and CD3 antibodies. A clustering of NKT cells was observed in CFTR<sup>-/-</sup> mice (**Fig. 5 A, C**), in contrast to the lung tissue of wild type (WT) mice (**Fig. 5 B, D**). NKT cell accumulated in areas of submucosal glands of CFTR<sup>-/-</sup> mice, identified by PAS staining (**E**) in subsequent tissue sections. Submucosal glands of WT mice did not show this accumulation.

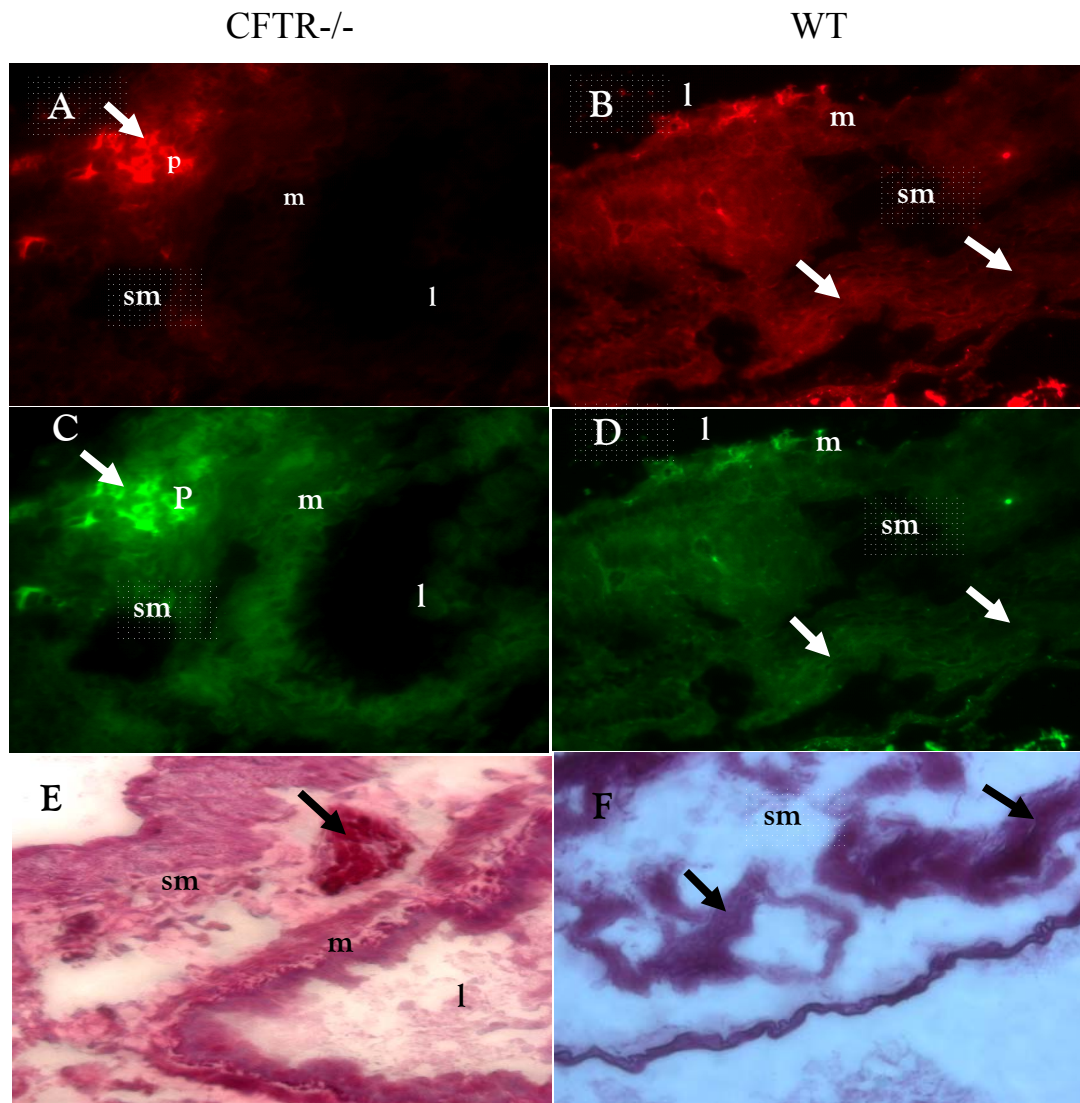


**Fig. 5. NKT cells accumulate around submucosal glands in 12 weeks old CFTR<sup>-/-</sup> mice.** Sequential tissue sections were stained for NKT cells with the mABs NK1.1 (**A, B**) and CD3

(C, D), followed by a second antibody, coupled to Cy3 (A, B) and Cy2 (C, D). Submucosal glands (**arrow**) were identified by PAS staining in CFTR<sup>-/-</sup> mice (E) and wild type (WT) mice (F). **l**: lumen of the bronchi; **m**: mucosal tissue; **P**: NKT cells; **sm**: submucosal tissue. Color change between E and F is a result of the tissue structure. Original magnification: 400X .

Another example supporting the co-localization of NKT cells with submucosal glands in 12 weeks old CFTR<sup>-/-</sup> mice is shown in **Fig. 6**.

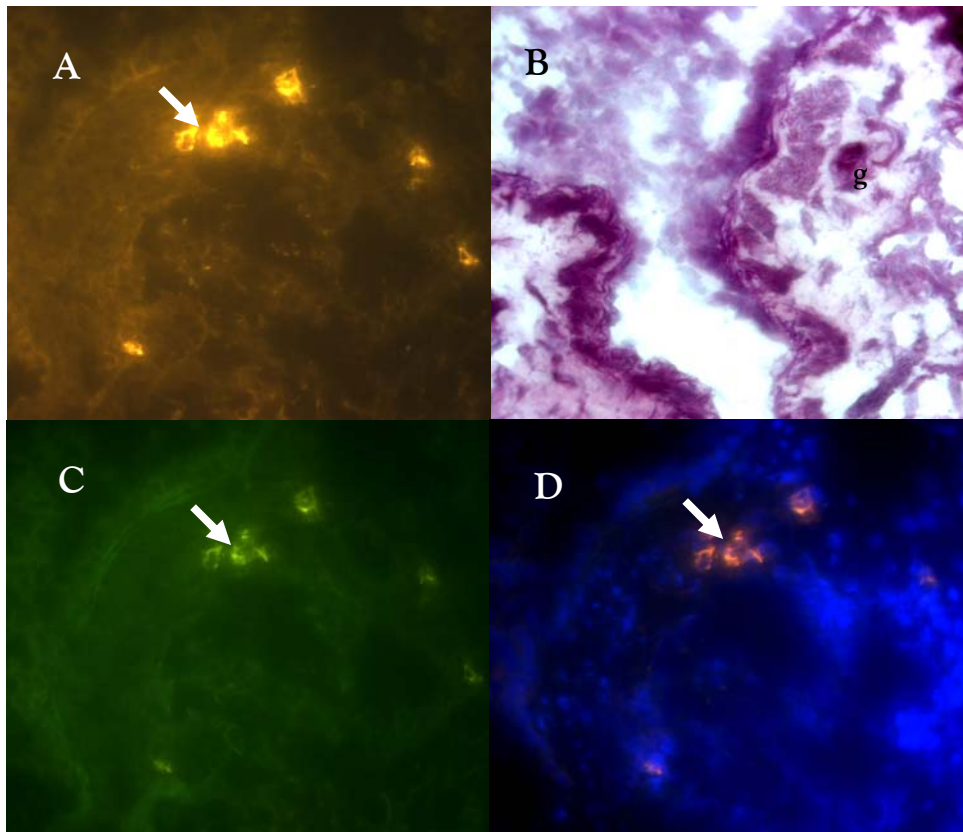


**Fig. 6. NKT cells accumulate around submucosal glands of 12 week old CFTR<sup>-/-</sup> mice.** NKT cells (**arrow**) were stained with the mAb NK1.1 (A) and CD3 (C), followed by a second antibody, coupled to Cy3 and Cy2. **D**: superposition of A and C with DAPI stain for cell nuclei. **B**: PAS-stained submucosal gland (**g**; **arrow**) of a subsequent tissue section. Original magnification: 400X .

When the number of NKT cells was counted in tissue sections of CF and WT mice, a significant increase in NKT cell numbers was observed in 12 weeks old CFTR<sup>-/-</sup> mice compared to WT mice (Fig. 7) (p=0.0006).

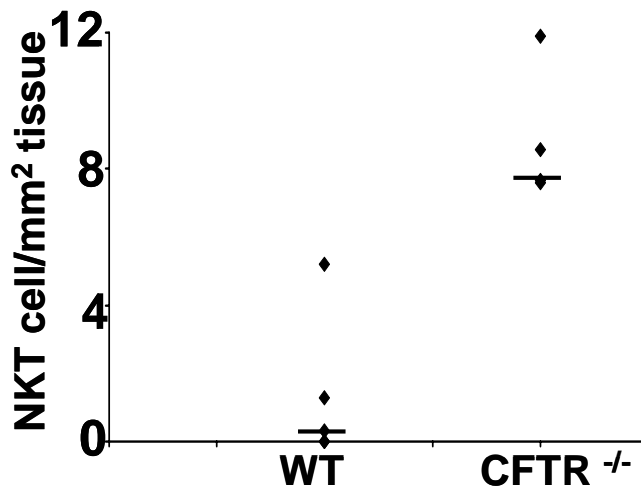


**Fig. 7. NKT cells are increased in lung tissue of 12 weeks old CFTR<sup>-/-</sup> mice.** Fluorescent labeled NKT cells were counted in lung tissue sections of 4 wild type (WT) and 4 CF mice. Values (◇) represent means of NKT cells counted in 4-10 single tissue areas per mouse.

### 3.2 NKT cell accumulation progresses with the age of CFTR<sup>-/-</sup> mice.

Significant clustering of NKT cells were also detected in 28 weeks old CFTR<sup>-/-</sup> mice (Fig 8 A, C, G), but not in normal mice (Fig. 8 B, D, H). NKT cells were located around submucosal glands, identified by PAS staining (I) in subsequent tissue sections. Again, submucosal glands of WT mice did not show this accumulation. Submucosal glands of CFTR<sup>-/-</sup> mice were enlarged (I) in comparison to WT mice and increased in numbers (data not shown).

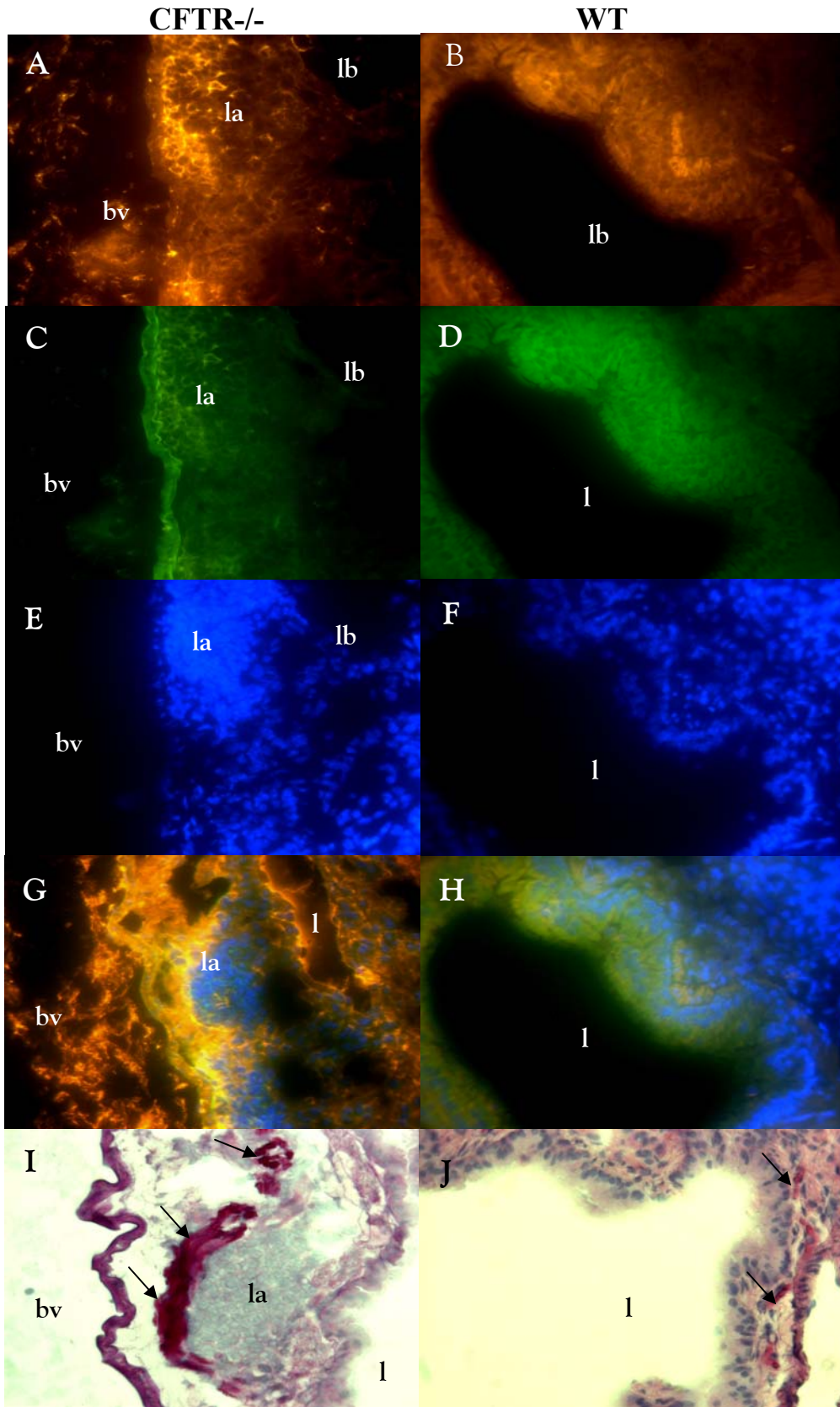




**Fig. 8. NKT cells numbers increased around submucosal glands in 28 weeks old CFTR<sup>-/-</sup> mice.** NKT cells were stained with the monoclonal antibody NK1.1 (A, B) and CD3 (C, D), followed by a second antibody, coupled to Cy3 (A, B) and Cy2 (C, D). Cell nuclei were stained with DAPI (E, F). G, H: superposition of A, C and E, and B, D, F, respectively. Submucosal glands (arrow) were identified by PAS staining in CFTR<sup>-/-</sup> mice (I) and 34 week old wild type (WT) mice (J). l: lumen of the bronchi; bv: blood vessel; lm: Lymphocyte aggregates in respiratory submucosal glands. Original magnification: 400X

When the number of NKT cells was counted in tissue sections of CF and WT mice, the increase in NKT cell numbers was even higher than that observed in 12 weeks old CFTR<sup>-/-</sup> mice (Fig. 9), suggesting that the CF defect triggers a progressive innate immune response (p=0.0003).

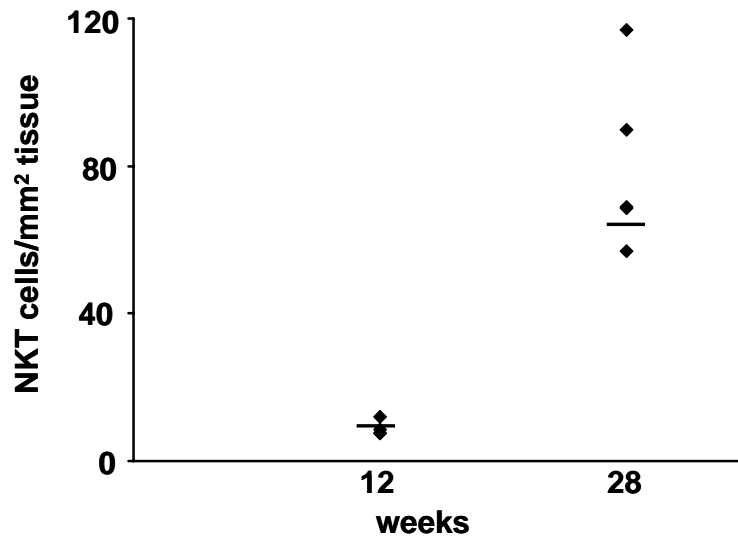


**Fig. 9. NKT cells expression is progressive with the age in CFTR<sup>-/-</sup> mice.** Fluorescent labeled NKT cells were counted in lung tissue sections of 12 weeks and 28 weeks old CFTR<sup>-/-</sup>. Values (◇) represent means of NKT cells counted in 4-10 single tissue areas per mouse. Four mice per age were investigated.

This notion was further corroborated when different sections of lung tissue of 12 week and 28 week old CFTR<sup>-/-</sup> mice was stained for NKT cells (Fig. 10). In 12 week old CFTR<sup>-/-</sup> mice, NKT cells were localized around submucosal glands of bronchi, but not in smaller bronchioli (Fig. 10 B), whereas in 28 week old CFTR<sup>-/-</sup> mice, NKT cells were also seen in the periphery of the lung including alveolar septa (Fig. 10 A). In the 28 week old mice, particularly high NKT cell numbers were present in areas of bronchial divisions (Fig 10 C-F).



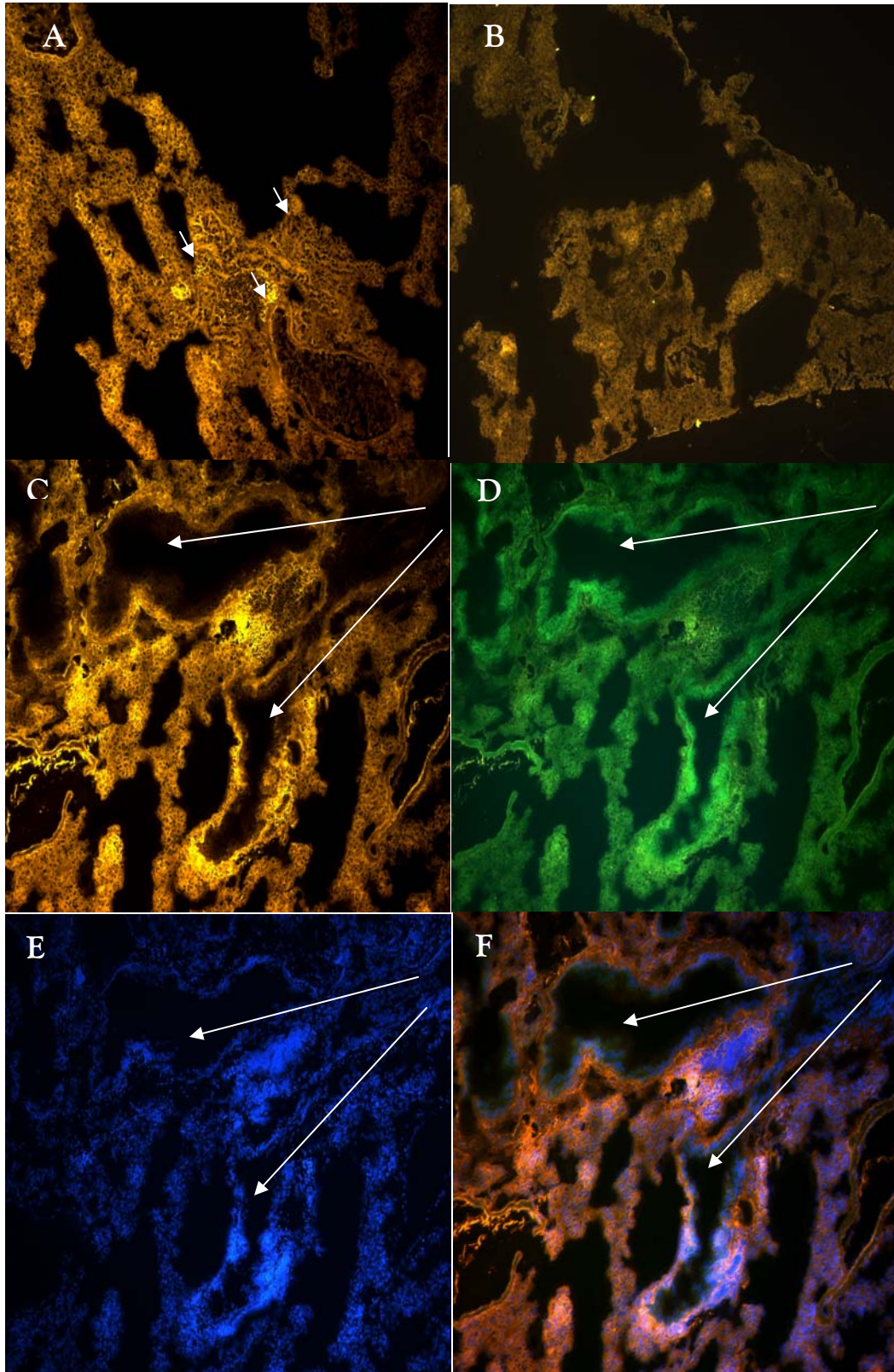


**Fig. 10. NKT cells in periphery and in areas of bronchial divisions in 28 week old CFTR<sup>-/-</sup> mice.** NKT cells were stained with the mAB NK1.1 and a second antibody, coupled to Cy3 (**A, B, C**) and with a mAB to CD3 and by a second antibody coupled to Cy2 (**D**). Cell nuclei were stained with DAPI (**E**). **F**: superposition of **C, D**, and **E**. NKT cells were identified (**arrow**) in 28 week old CFTR<sup>-/-</sup> mice (**A**), but not in 12 week old CFTR<sup>-/-</sup> mice (**B**) and particularly high NKT cell numbers were present in the area of bronchial divisions B1, B2, B3 (**arrows**) of the upper lobe bronchi of 28 week old CFTR<sup>-/-</sup> mice (**C-F**). la: Lymphocyte aggregates. Original magnification:100X.

### 3.3. Accumulation of macrophages and neutrophils in CFTR<sup>-/-</sup> mice.

Activated mouse V $\alpha$ 14 NKT cells rapidly secrete cytokines and chemokines, particularly interferon  $\gamma$  (INF-  $\gamma$ ) and IL-4, supporting T helper 1 (TH1) cell differentiation at an early stage and TH2 cell development at a later stage [52, 53, 60, 61]. To investigate whether NKT cell activation leads to the influx of macrophages and/or neutrophils, we stained lung tissue of CFTR<sup>-/-</sup> mice and controls for these effector cells. An increase in macrophage cell numbers was observed in the submucosa of CFTR<sup>-/-</sup> mice (**Fig. 11 A, C**). Only marginal macrophage numbers were present in WT mice (**Fig. 11 B, D**).

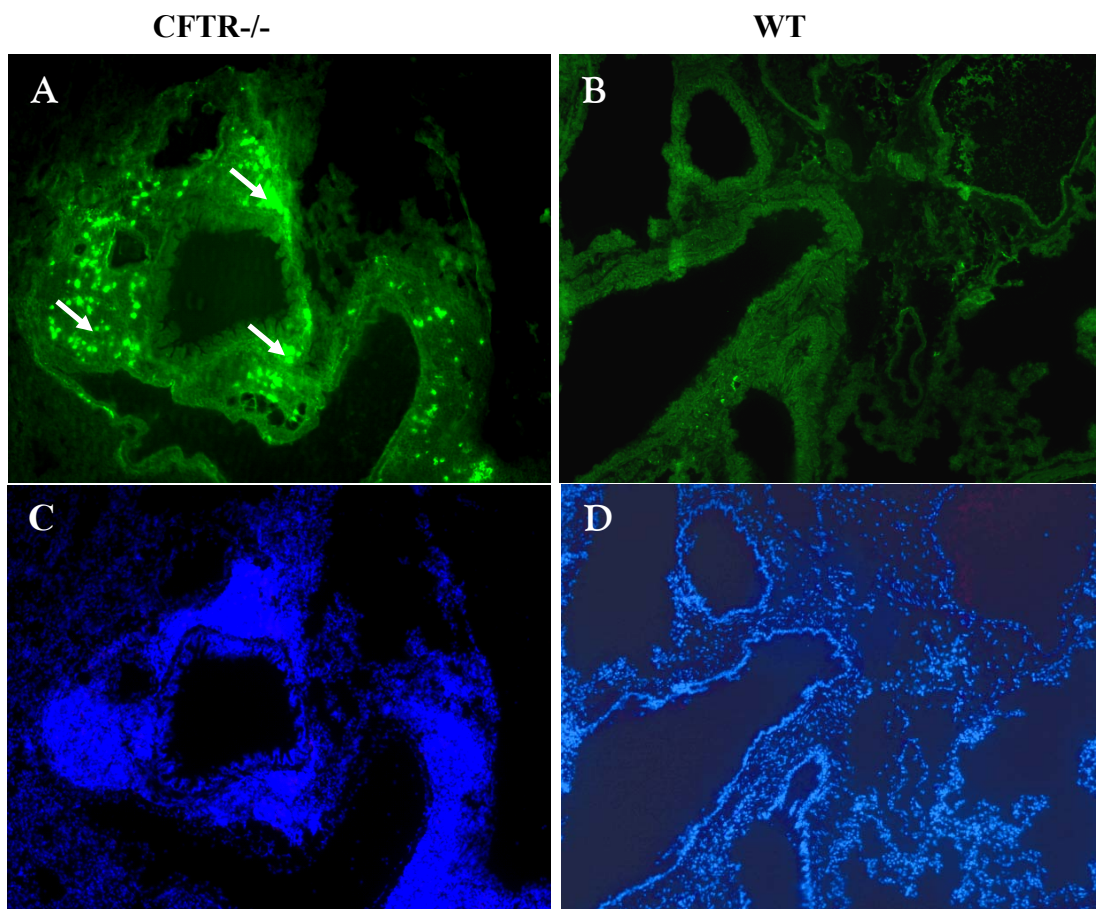




**Fig. 11** Accumulation of macrophages in submucosal lung tissue of 32 week old CFTR<sup>-/-</sup> mice. Macrophages (arrow) were stained with a mAB to murine CD68, followed by a second antibody, coupled to Cy2 (A, B), or stained with DAPI for cell nuclei (C, D). Macrophages were highly increased in CFTR<sup>-/-</sup> mice (A), compared to 52 week old wild type (WT) mice (B). Original magnification: 100X.

Similar results were observed when neutrophils were stained (Fig. 12).

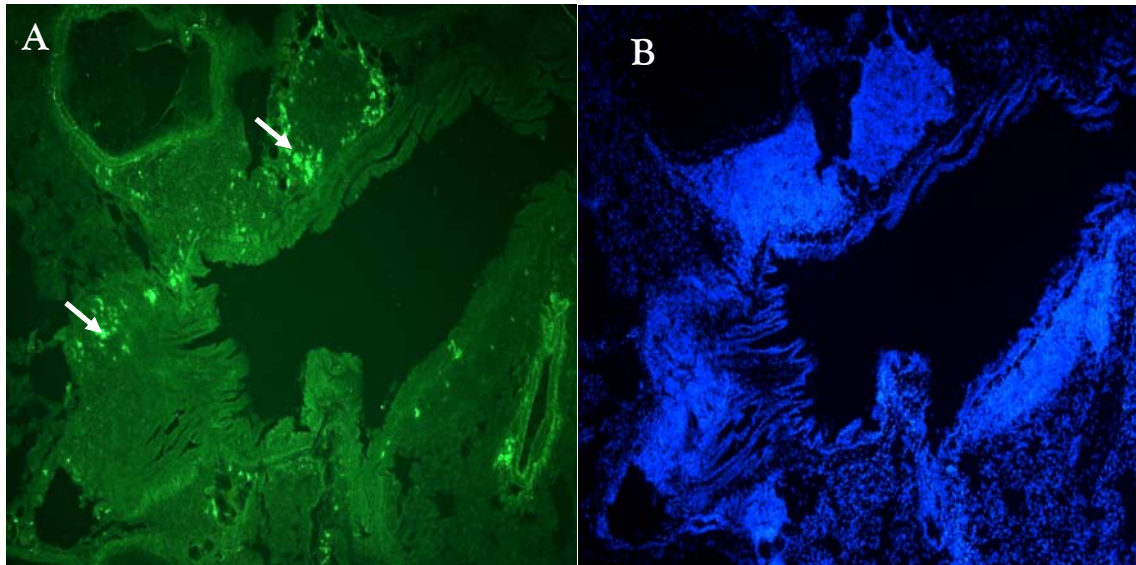


**Fig. 12.** Accumulation of neutrophils in the lung submucosa in 30 week old CFTR<sup>-/-</sup> mice. Neutrophils (arrow) were stained with a rat anti-mouse neutrophil antibody, followed by a second Cy2-coupled anti-rat antibody (A) or stained with DAPI for cell nuclei (B). Neutrophils were highly increased in CFTR<sup>-/-</sup> mice, compared to wild type mice (not shown; see fig. 14). Original magnification:100X.

To rule out that the observed macrophage/neutrophil clustering in the submucosa of CFTR<sup>-/-</sup> mice was due to lung infection, *P. aeruginosa*-infected C57Bl/6 wild type mice were stained for macrophages (**Fig 13**). Macrophages were predominantly clustering in the lung epithelium and in the airway lumen, however not observed in the submucosa.

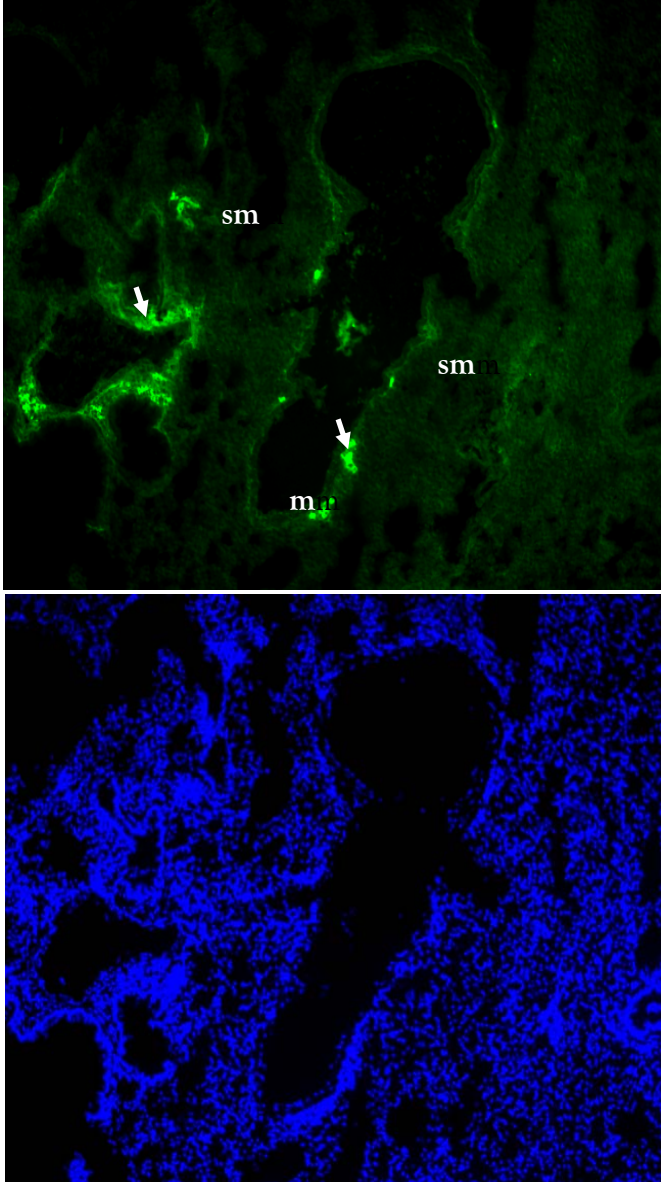


**Fig. 13. Macrophage clustering in the lung epithelium of 28 week old *P. aeruginosa*-infected wild type (WT) mice.** Macrophage (arrows) were stained with an mAb to murine CD68, followed by a second antibody, coupled to Cy2 (A) or stained with DAPI for cell nuclei (B). Macrophages were highly increased in the epithelium of *P. aeruginosa*-infected WT mice, but not in the submucosal tissue. **m**: mucosa; **sm**: submucosal tissue. Original magnification:100X.

In CFTR<sup>-/-</sup> mice, macrophage ( $p < 0.0001$ ) and neutrophil ( $p = 0.0015$ ) numbers increased with the age of the animals and were significantly different from these cell numbers in WT mice 52 weeks of age (Fig. 14).

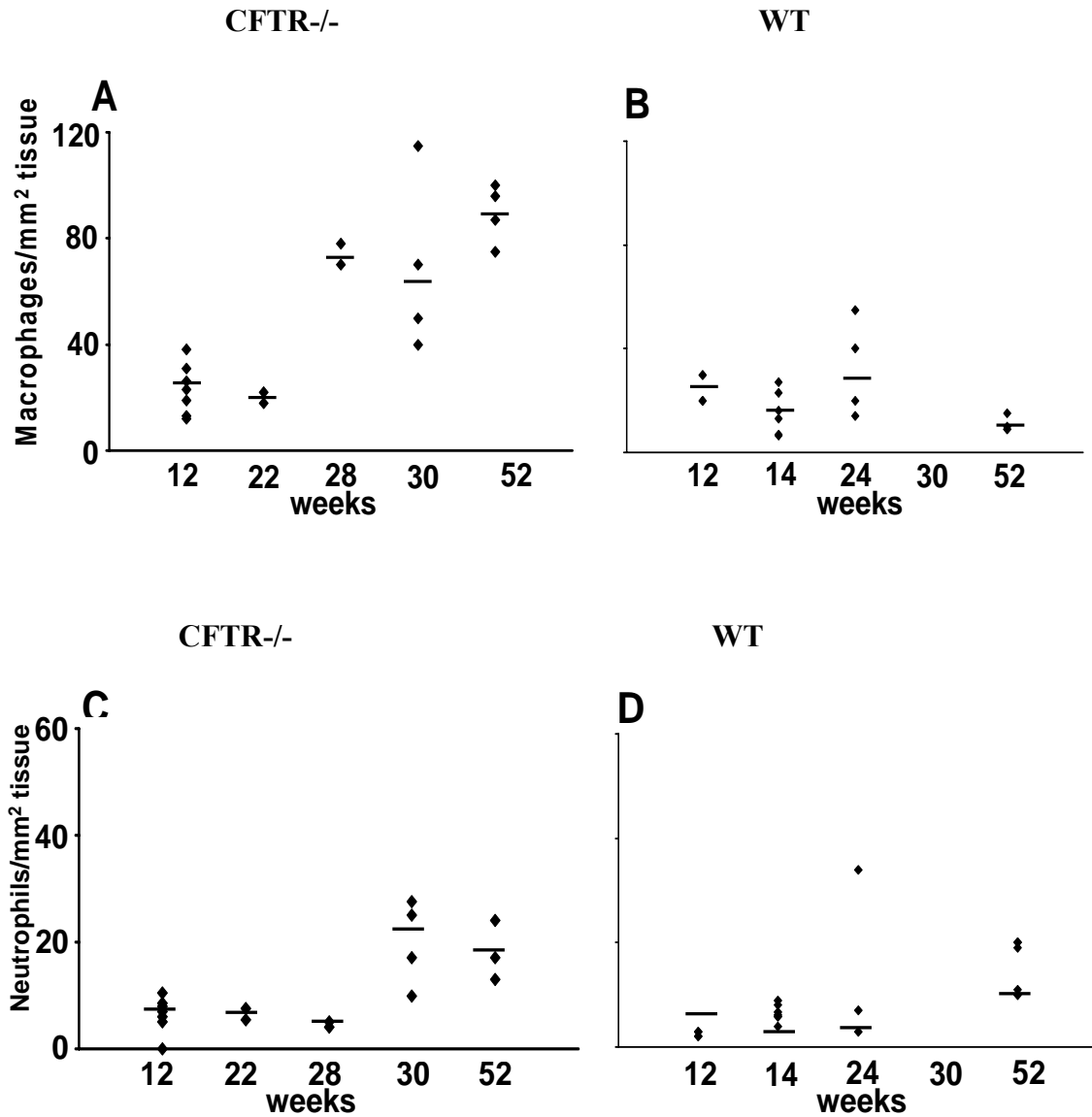


**Fig. 14. Macrophage and neutrophil numbers increased with the age of CFTR<sup>-/-</sup> mice.** Fluorescent labeled macrophages (A, B) and neutrophils (C, D) were counted in lung tissue sections of CFTR<sup>-/-</sup> mice and wild type (WT) mice of different ages. The number of macrophages significantly differed between CFTR<sup>-/-</sup> at 28 weeks of age and WT mice at 52 weeks of age. Neutrophil numbers were significantly different between the two groups at 52 weeks of age. Values (◇) represent means of Macrophages or neutrophils counted in 4-10 single tissue areas per mouse. A: 21 mice; B: 13 mice; C: 17 mice; D: 12 mice were investigated.

### 3.4. Accumulation of ceramide in lung tissue of CFTR<sup>-/-</sup> mice.

Since NKT cells recognize endogenous glycosphingolipids, such as isoglobotrihexosylceramide (iGb3) [56, 57], presented by the MHC class I-like CD1d protein, lung tissue sections of CFTR<sup>-/-</sup> mice and controls were stained with an antibody against ceramide. Indeed, in lung tissues of CFTR<sup>-/-</sup> mice, significantly increased concentrations of ceramide were expressed in the area of mucosal tissue (epithelium) and submucosal glands (Fig. 15 A) and in the periphery (not shown) compared to control tissues (Fig. 15 B).

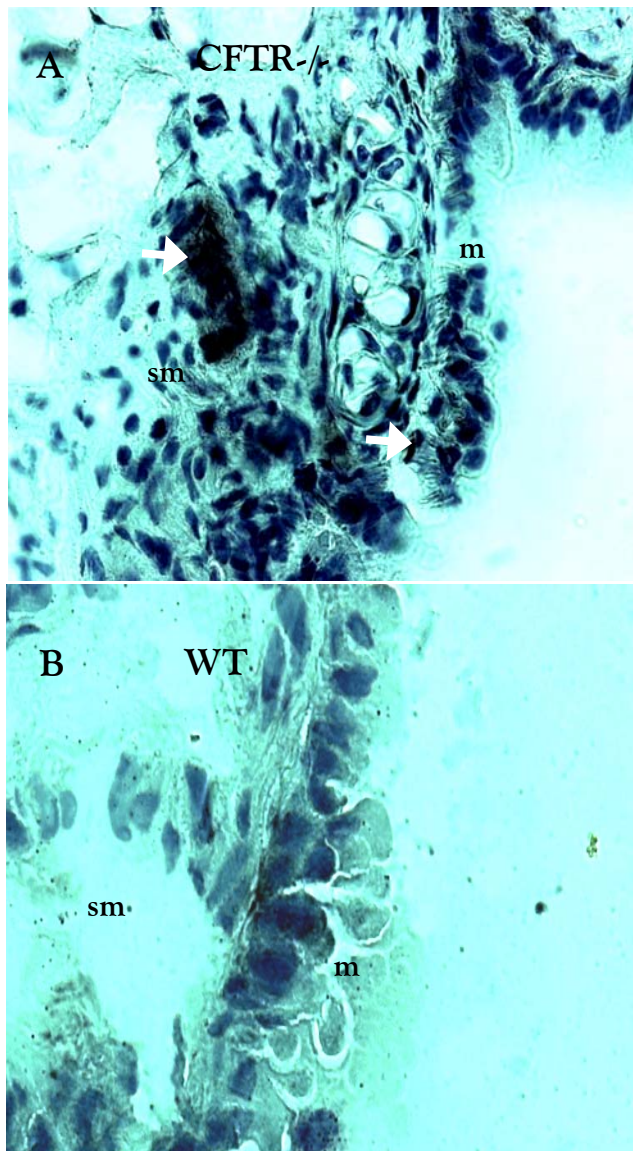


**Figure 15. Significantly increased concentrations of ceramide were present in mucosa and submucosal glands of CFTR<sup>-/-</sup> murine lungs. Ceramide (black areas, arrows) was stained with a mAB to ceramide in CFTR<sup>-/-</sup> mice (A) and wild type (WT) mice (B) followed by a second antibody, coupled to an anti-maus antibody-coupled to PAAP. m: mucosa; sm: submucosal tissue. Original magnification: 600X.**



### 3.5 Amitriptyline reduces ceramide expression and NKT cells in CFTR<sup>-/-</sup> mice.

To prove that the age-dependent NKT cell recruitment in CFTR<sup>-/-</sup> mice is correlated to ceramide overexpression, amitriptyline was intraperitoneally administered to CFTR<sup>-/-</sup> mice for 48 h before ceramide and NKT cell staining. Amitriptyline blocks acid sphingomyelinase (ASMase) which by cleaving sphingomyelin produces ceramide in cell membranes [62]. A significant reduction of ceramide (**Fig. 16**) and NKT cells (**Figs. 17, 18**) was observed in the lung tissues of 28 to 52 week old CFTR<sup>-/-</sup> mice (**p=0.0002**).

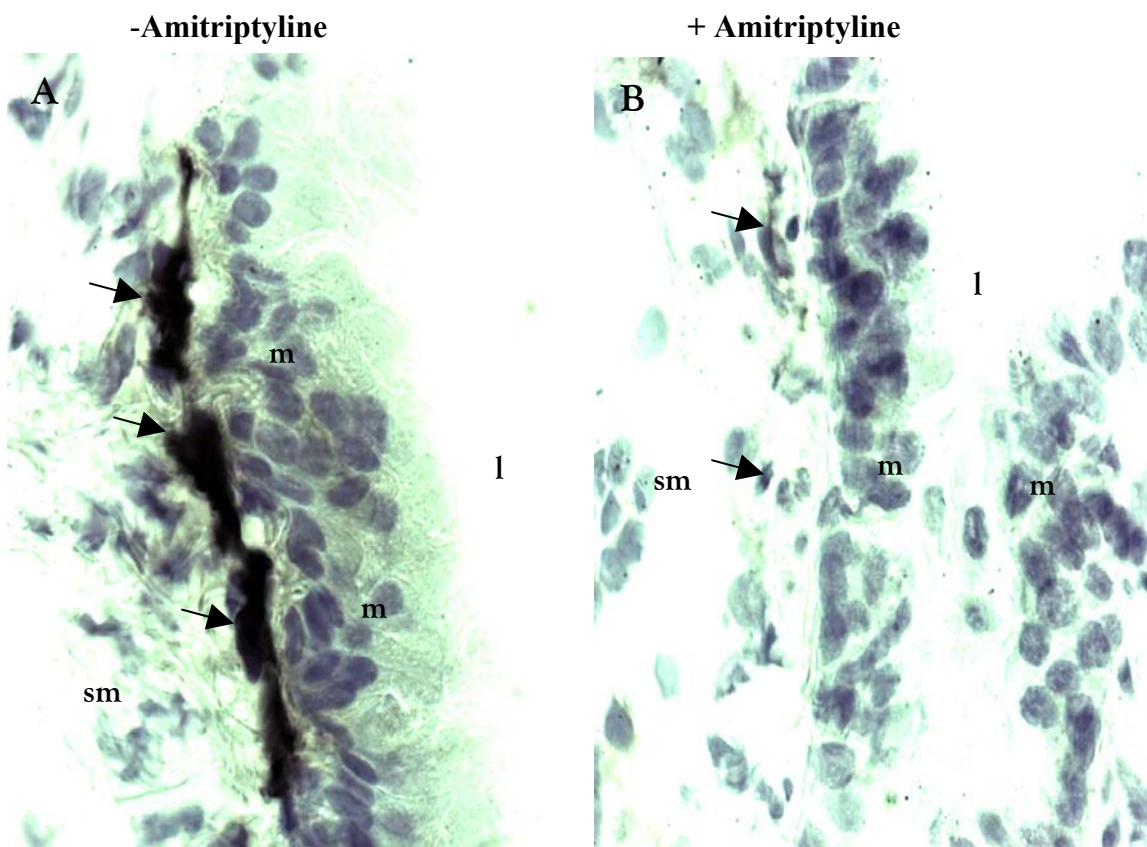


**Fig. 16. Amitriptyline reduces ceramide expression in the lung mucosa of CFTR<sup>-/-</sup> mice.** Ceramide (arrows) was stained with a mAB to ceramide in untreated (A) and amitriptyline treated (B) CFTR<sup>-/-</sup> mice, followed by a second antibody coupled to PAAP. **m**: mucosa; **sm**: submucosa; **l**: lumen of the bronchi. Original magnification: 600X.

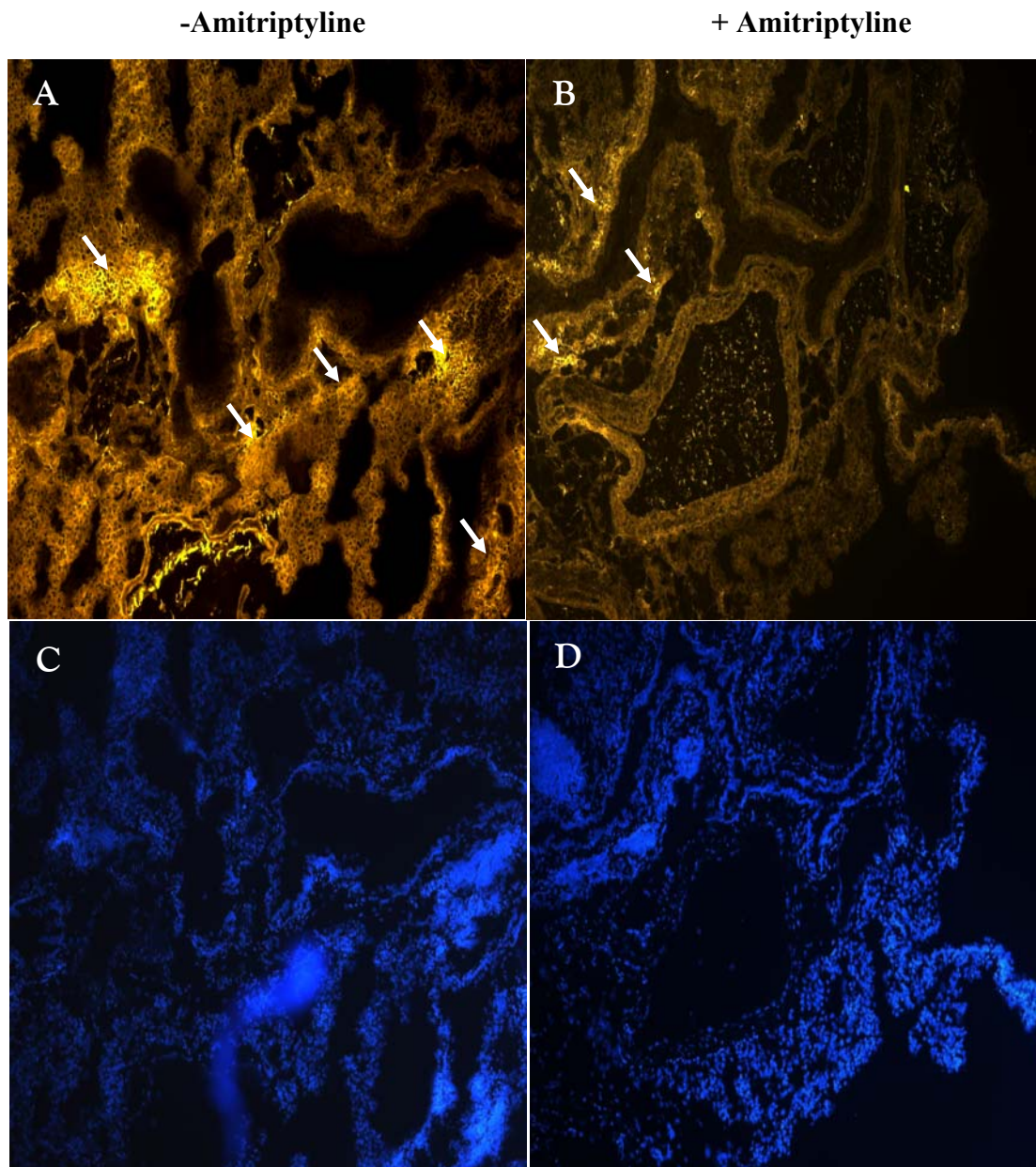


**Fig. 17. Amitriptyline reduces NKT cell numbers in the submucosa of 28 week old CFTR<sup>-/-</sup> murine lungs.** NKT cells were stained with the mAb NK1.1 (**A, B**), followed by a second antibody, coupled to Cy3, or stained with DAPI (**C, D**). Numbers of NKT cells (**arrows**) decreased in amitriptyline treated CFTR<sup>-/-</sup> mice (**B**), compared to untreated CFTR<sup>-/-</sup> mice (**A**). Original magnification: 100X.



Furthermore, clustering of NKT cells around submucosal glands was not any more present in amitriptyline treated CFTR<sup>-/-</sup> mice. When NKT cells were counted in amitriptyline treated and untreated 28 week old CFTR<sup>-/-</sup> mice, NKT cells decreased significantly ( $p=0.0002$ ). (**Fig. 18**). Similar results were observed when macrophages were stained in CFTR<sup>-/-</sup> amitriptylin treated mice (**Fig. 18**) ( $p=0.001$ ). In contrast, CD4<sup>+</sup> T cells did not decrease (**Fig. 24**) ( $p=0.19$ ). Taken together these findings demonstrate a correlation between defective CFTR expression, increased ceramide expression and increased NKT cell recruitment.

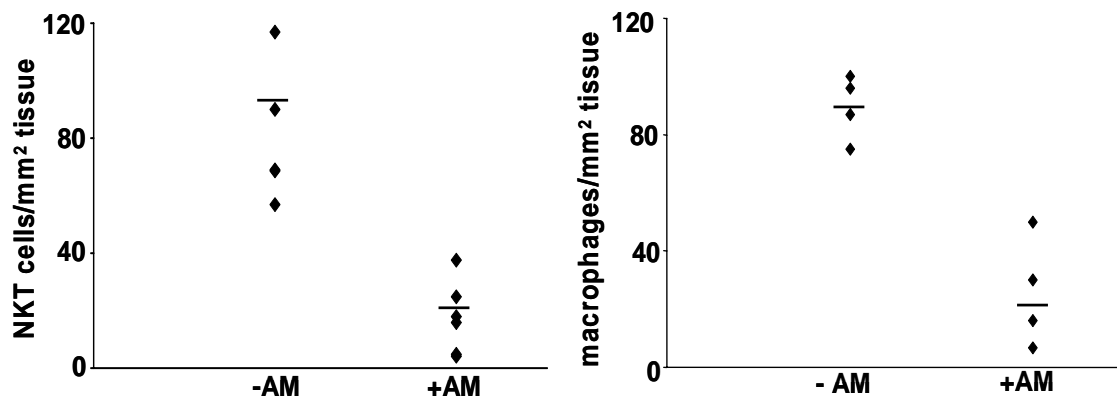


**Fig. 18. Amitriptyline decreases NKT and macrophage cell numbers in 28 week old CFTR<sup>-/-</sup> mice.** Fluorescence-labeled NKT cells and macrophages were counted in lung tissue sections of amitriptyline treated and untreated CFTR<sup>-/-</sup> mice. A significant difference was found for NKT cells ( $p=0.0002$ ) and macrophages ( $p=0.001$ ). Values ( $\diamond$ ) represent means of NKT cells or macrophages, counted in 4-10 single tissue areas per mouse. For NKT cells 9 mice, for macrophages 8 mice were investigated.

### 3.6. Accumulation of NKT cells in intestinal tissues of CFTR<sup>-/-</sup> mice.

Since the CF defect is also expressed in pancreas, liver and the intestinal tract, the respective tissues derived from 34 week old CFTR<sup>-/-</sup> and the respective wild type mice were stained for NKT cells (**Fig. 19**). High NKT cell expression was observed in the mucosal lamina propria of jejunum (**A**), ileum (**C**) and colon (**E**) of CFTR<sup>-/-</sup> mice but not in the respective tissues of control mice (**B, D, F**). The results further suggest that the observed NKT cell recruitment in CFTR<sup>-/-</sup> mice is correlated to the basic CF defect. Increased cell

numbers of macrophage, neutrophils, NK cells, CD4+ or CD25+ lymphocytes were not observed in the 34 week old CFTR<sup>-/-</sup> mice in the investigated intestinal tissues (not shown).

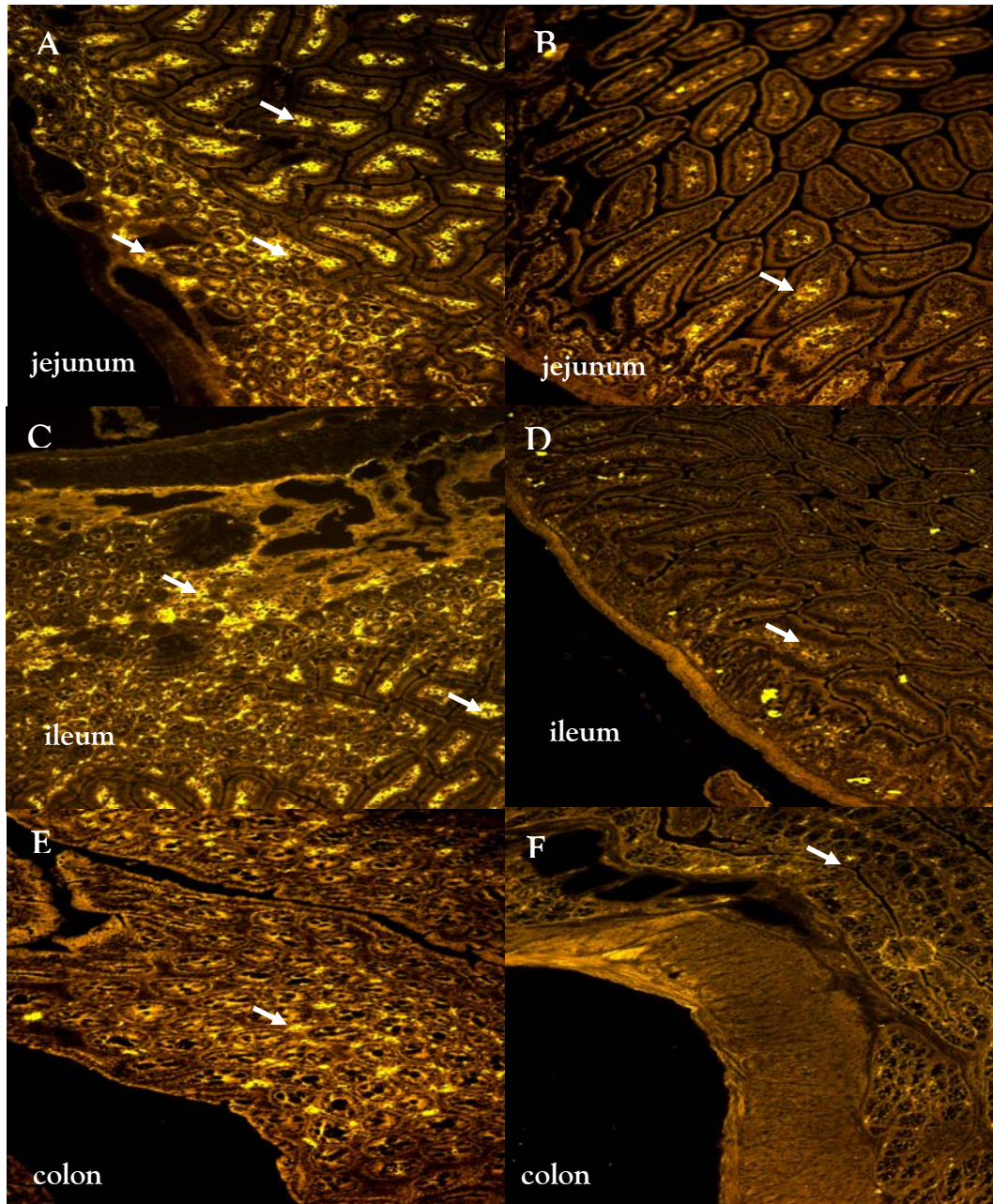


**Fig. 19. High NKT cell expression in the mucosal lamina propria of jejunum, ileum and colon of 34 week old CFTR<sup>-/-</sup> mice. NKT cells were stained with the mAB NK1.1 (A-F), followed by a second antibody, coupled to Cy3. Original magnification:100X.**

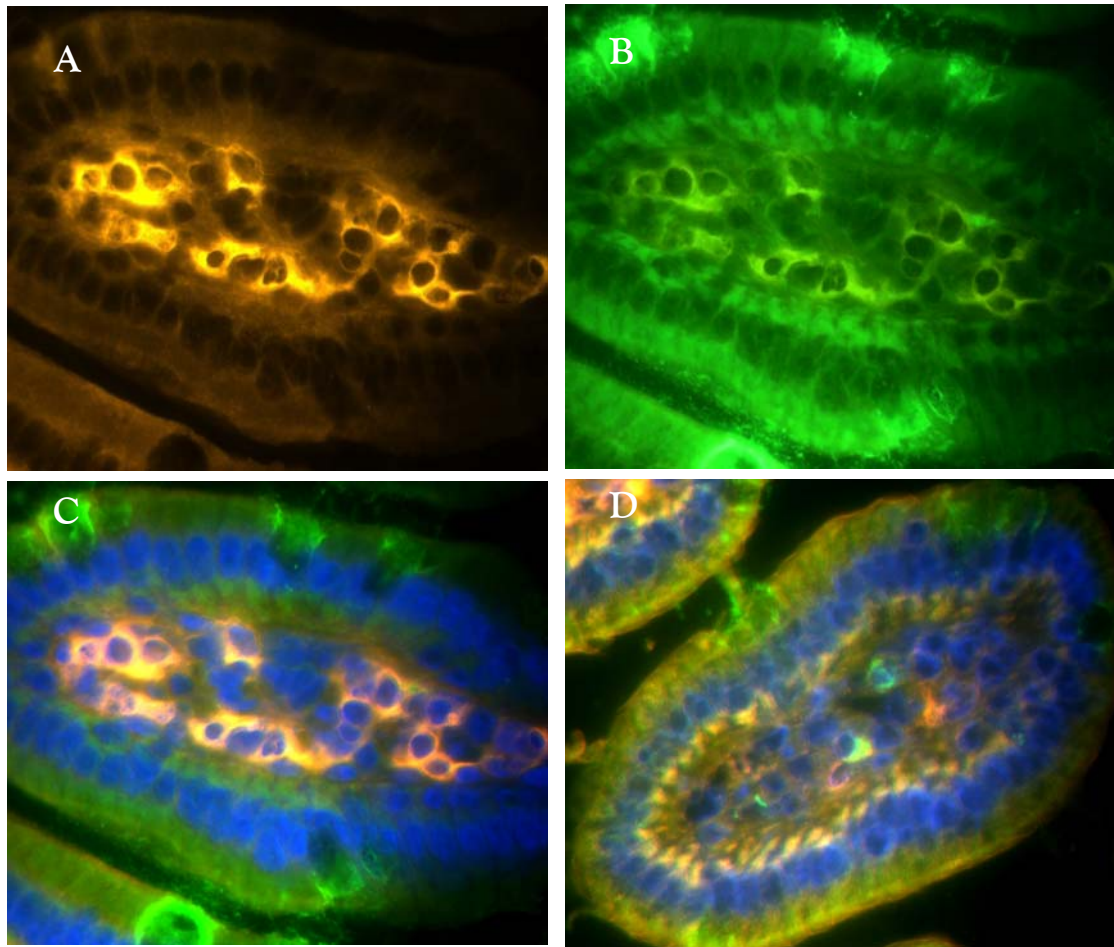


**Fig. 20. High NKT cell expression in the mucosal lamina propria of jejunum of 34 week old CFTR<sup>-/-</sup> mice (A-C) compared to wild type mice (D).** NKT cells were stained with the mAB NK1.1, followed by a second antibody, coupled to Cy3 (A) or an mAB against CD3, followed by a second antibody, coupled to Cy2 (B). C: superposition of A and B plus DAPI staining. D: superposition of wild type staining using mAB to NK1.1 and CD3 as in A and B plus DAPI staining. Original magnification:1000X .



### 3.7 Accumulation of other immunocompetent cells in respiratory submucosal glands of CFTR<sup>-/-</sup> mice.

Whereas in 12 week old WT mice minimal CD4<sup>+</sup> T cells were present, this cell type was increased in 12 week old CFTR<sup>-/-</sup> mice (**Fig. 21**). PAS staining revealed that the cell accumulation was located around submucosal glands (**Fig. 21 C, D**). Similar differences were observed regarding CD25<sup>+</sup> T cells (not shown). No difference in cell numbers was observed with regard to NK cells between WT and CFTR<sup>-/-</sup> mice (data not shown).

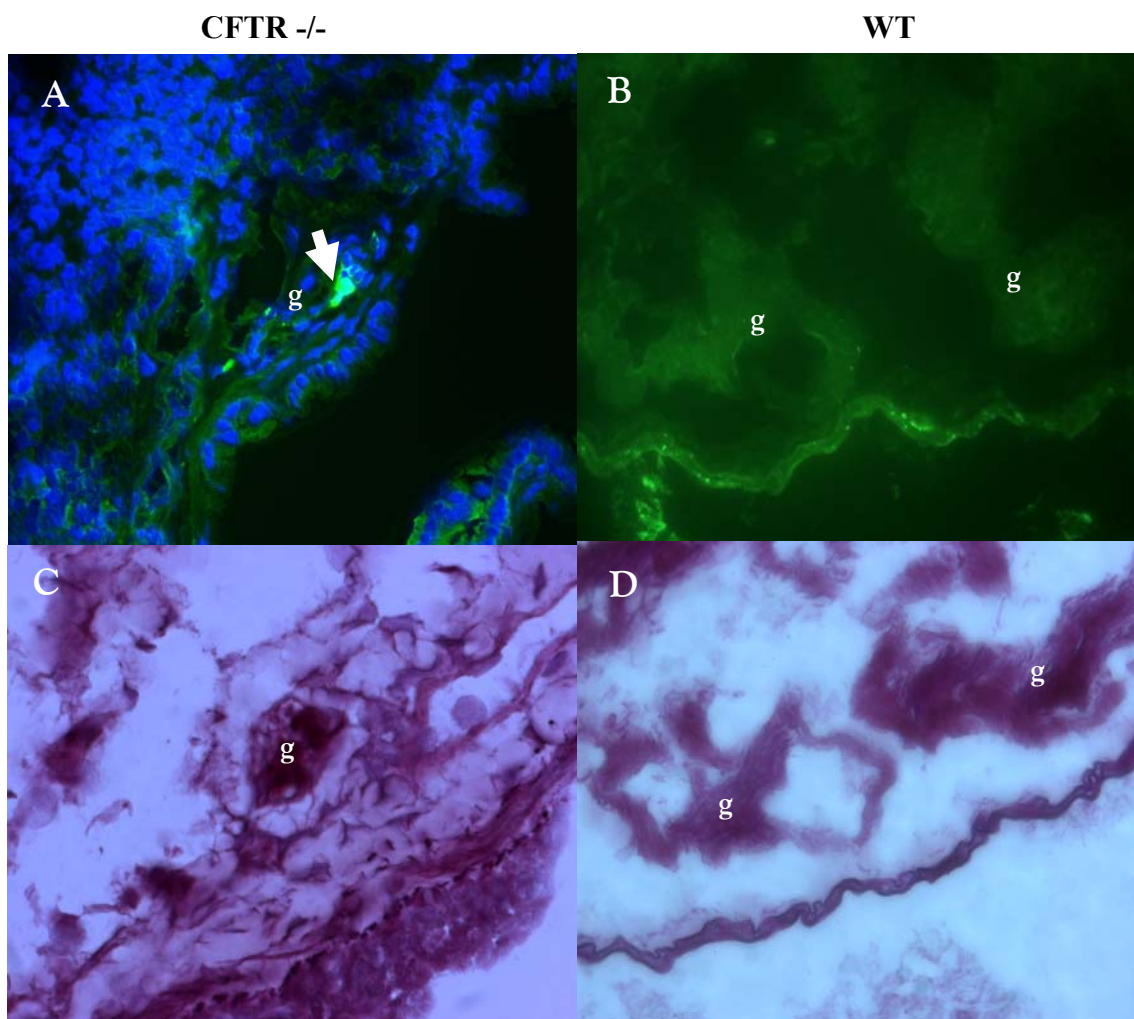


**Fig. 21. CD4<sup>+</sup> T cells were present in 12 weeks old CFTR<sup>-/-</sup> mice.** CD4<sup>+</sup> T cells were stained with mAB to CD4, followed by a second antibody coupled to Cy2 (**A, B**). Glands (**g**) were stained with PAS (**C, D**). CD4<sup>+</sup> T cells (**arrow**) were increased around submucosal glands in 12 week old CFTR<sup>-/-</sup> mice (**A, C**), compared to wild type mice (**B, D**). Original magnification: 400X.

As with NKT cells and macrophages, the numbers of CD4+ and CD25+ T cells were further increased in 28 week old CFTR<sup>-/-</sup> mice (**Fig. 22**). Particularly high CD4+ and CD25+ T cells numbers were present in areas where bronchial lobes divide. Amitriptyline had no influence on CD4+ cell numbers (**Fig. 23**) ( $p=0.19$ ).

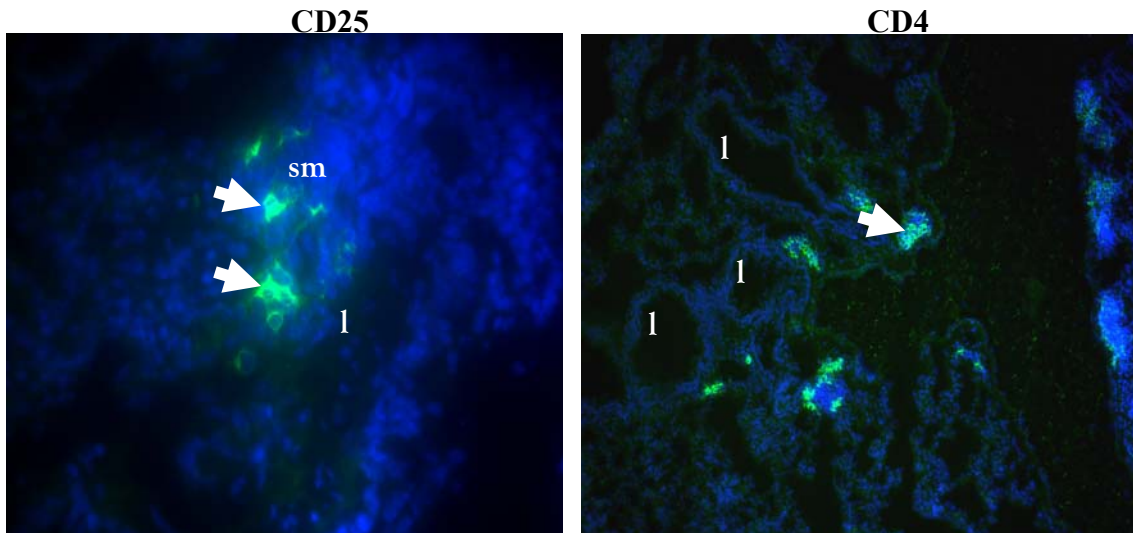


**Fig. 22 Accumulation of CD25+ and CD4+ T cells in the respiratory submucosa of 28 week old CFTR<sup>-/-</sup> mice.** CD25+ and CD4+ T cells (**arrows**) were stained with specific mABs, followed by a second antibody, coupled to Cy2+. Sections were also stained with DAPI for cell nuclei. CD25+ and CD4+ T cells were high increased around submucosal glands compared to wild type mice (**data not shown**). **l**: lumen of the bronchi; **sm**: submucosal tissue. Original magnification: CD25 400X; CD4+T cells100X.

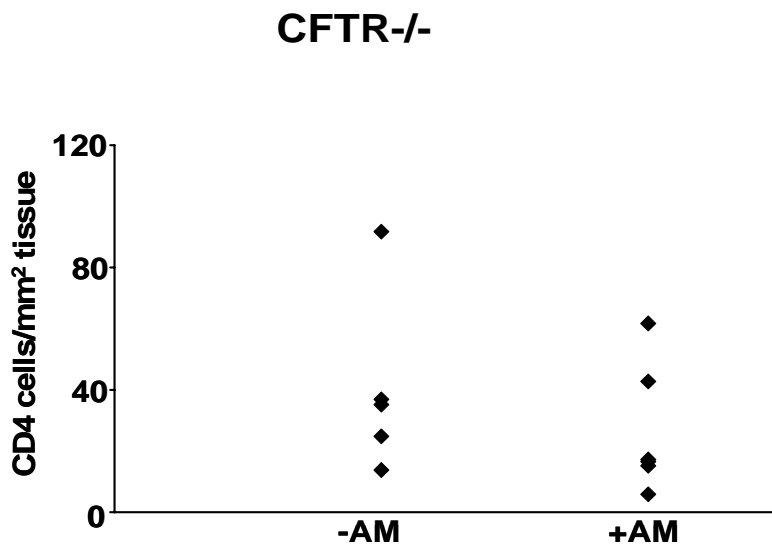


**Fig. 23. Amitriptyline has no impact on CD4+ T cells numbers in 28 week old CFTR<sup>-/-</sup> mice.** Fluorescence labeled CD4+ T cells were counted in lung tissue sections of 28 weeks old untreated and amitriptylin treated CFTR<sup>-/-</sup>. No significant differences were seen ( $p=0.19$ ).

### 3.8. Lymphocyte aggregates are present around respiratory submucosal glands of CFTR<sup>-/-</sup> mice.

The described accumulation of cells of the innate immune system (NKT cells, macrophages, neutrophils) and the acquired immune system (CD4<sup>+</sup>, CD25<sup>+</sup> T cells) represents a Lymphocyte Aggregate (LA) (Fig. 24). The LA was localized by immunofluorescent staining in the lung tissue of CFTR<sup>-/-</sup> mice, predominantly around submucosal glands, but not in normal WT mice (Fig. 25). Additionally, LAs were present in the area of bronchial divisions suggesting a concerted action, possibly directed against the basic defect in CF, i.e., mutated or absent CFTR. LAs were not observed in normal mice, regardless of their age.

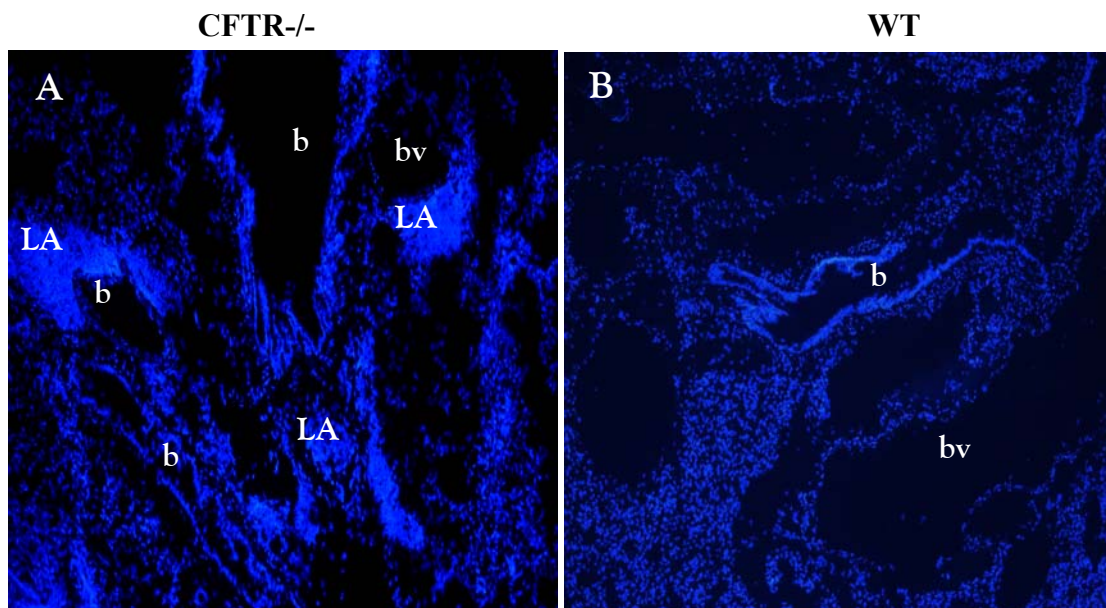


**Fig. 24** Several Lymphocyte Aggregates (LA) were present in submucosal lung tissues of 28 week old CFTR<sup>-/-</sup> mice. Lung tissue sections of 28 week old CFTR<sup>-/-</sup> mice (A) and 52 week old wild type (WT) mice (B) were stained with DAPI for cell nuclei. The LAs were present in CFTR<sup>-/-</sup> mice (A), but not in wild type mice (B). **b**: bronchi.; **bv**: blood vessel. Original magnification: 100X.



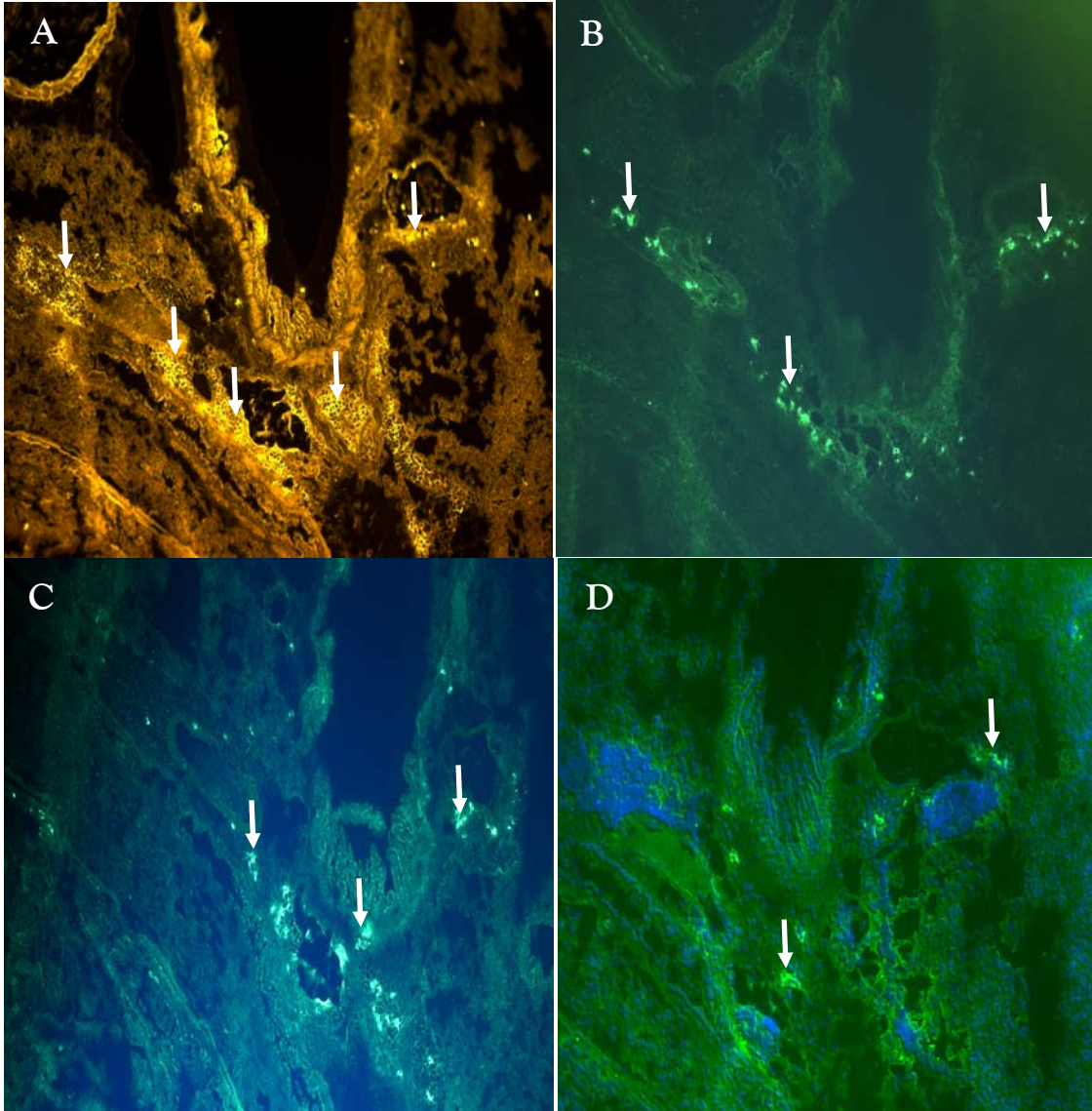


**Fig. 25 Lymphocyte Aggregates (LA) in lung tissue of CFTR<sup>-/-</sup> mice.** Subsequent sections of a CF mouse were stained with mAB against NKT cells (A), macrophages (B), CD4<sup>+</sup> T cells (C) and NK cells (D). Original magnification:100X.

#### 4. DISCUSSION

The data of the present study demonstrate first the first time a correlation between defective CFTR expression, increased ceramide expression and an increased recruitment of cells of the innate and adaptive immune system in CF mouse strains. CFTR has been demonstrated to be primarily expressed in submucosal glands of human airways [14] and it is predominantly around submucosal glands that high ceramide expression and aggregation of immunocompetent cells including NKT cells was observed in different CF mouse strains (**Fig. 5, 6, 8, 15**). In addition, NKT cell numbers were highly increased in intestinal tissues of CF mice which express CFTR (**Fig. 19, 20**). Furthermore, ceramide and NKT cells were significantly increased in the periphery of the lungs of CFTR<sup>-/-</sup> mice (**Fig. 10 B**).

Why ceramide expression is abnormally high in CF tissues is unclear. Ceramide is synthesized through a *de novo* pathway involving serine palmitoyl-CoA transferase and ceramide synthase or from membrane sphingomyelin breakdown by the secretory isoform of neutral and acid sphingomyelinase (ASMase) [62]. It has multiple biochemical effects including the stimulation of apoptosis [63]. Indeed, by blocking ASMase with amitriptyline, ceramide concentrations decreased in lung tissues of CFTR<sup>-/-</sup> mice (**Fig. 16**).

The observation that amitriptyline treatment of CFTR<sup>-/-</sup> mice, in addition to ceramide reduction, also significantly resolved NKT cell accumulation and reduced NKT cell numbers (**Fig. 17**), suggests a link between ceramide and NKT cells. NKT cells recognize exogenous and endogenous glycolipids, presented by the MHC class I-like CD1d protein via their conserved, semi-invariant V $\alpha$ 14-J $\alpha$ 18/V $\beta$ 8 TCR [54-59] (**Fig. 3**). Structural studies reveal, that the ceramide tail of various glycolipids fits perfectly in the binding groove of CD1d [54]. It is intriguing to speculate that the observed ceramide accumulation in tissues of CF mice is indeed an accumulation of a self lipid antigen containing ceramide, whose carbohydrate component is unknown. A candidate for such a self glycolipid antigen is isoglobotrihexosylceramide (iGb3) (**Fig. 3**), which has been suggested to be primarily recognized by NKT cells in mice and men [56, 57].

A link to the existing notions concerning the CF pathophysiology may relate to early studies showing that glycoconjugates from respiratory epithelial cells of CF patients were



more sulfated and fucosylated and undersialylated than respective control glycoconjugates [64-66]. These abnormalities have been explained as a consequence of defective acidification of the trans-Golgi network in CFTR expressing cells [67]. A more basic pH could modify the activity of glycosyltransferases leading to the observed changes [68]. However, also a shift to a more acidic pH could result in undersialylation of glycoconjugates. Indeed, hyperacidification of endosomal organelles in CF lung epithelial cells has been demonstrated [68] and explained as a consequence of diminished CFTR inhibition on sodium transport [69]. The internal pH values in CF cell lines at pH 6.0 were 0.7 and 0.6 pH units lower than in corrected cell lines ( $P=0.0001$ ) [69]. Lysosomal hyperacidification may possibly affect also the enzymes which degrade glycosphingolipids. Provided that  $\alpha$ -Galactosidase A is inhibited, an accumulation of iGb3 may occur which would be attractive for NKT cells (**Fig. 3**). The present study opens the possibility to test the hypothesis that ceramide is linked to glucose and galactose to form iGb3, and if so, to determine the concentration of iGb3 in intestinal tissues of CF mouse strains and compare it with that in normal murine intestine.

In parallel with the increase of NKT cell numbers with increasing age of CFTR<sup>-/-</sup> mice (**Fig. 9**), an age-dependent significant increase in macrophage and neutrophil cell numbers, present at submucosal glands in the respiratory tract of CFTR<sup>-/-</sup> mice was observed (**Fig. 14**). Since activated V $\alpha$ 14 NKT cells produce large amounts of cytokines within hours of primary stimulation and can drive immune responses in both pro- and anti-inflammatory directions [52, 53, 61] (**Fig. 4**), it is possible that the age-dependent increase of macrophages and neutrophils is due to the increased NKT cell numbers. However, it is equally possible that these effector cells are attracted to non-functional CFTR cells in an NKT cell-independent manner. Nevertheless, normalization of ceramide expression in amitryptilin treated CFTR<sup>-/-</sup> mice which reduced NKT cell, macrophage and neutrophil numbers and prevented their accumulation around submucosal glands significantly, support the link between NKT cell, macrophage and neutrophil accumulation. To differentiate between these two possibilities, the generation of a Hexb<sup>-/-</sup>-CFTR<sup>-/-</sup> mouse strain would be helpful. Alternatively, treatment of CFTR<sup>-/-</sup> mice with the mAB NK1.1 may dissolve this issue.

Also other investigators have reported widespread pathology in CF mice. Increased inflammatory cells numbers in the lamina propria of pathogen-free raised CFTR<sup>-/-</sup> mice [32] and abnormal regulation of inflammation in lungs of *cftr*<sup>G551D</sup> mice [38] has been demonstrated. Additionally, in comparison with age-matched wild-type littermates, alveolar architecture of *Cftr*<sup>-/-</sup> mice was compromised (**Fig. 26**) (36, 70). The authors reported on patchy areas of acinar dilation, typical of obstructive lung disease, in all *Cftr*<sup>-/-</sup> animals at all ages, progressive interstitial disease, and an increase in collagen and in the number of interstitial fibroblasts (36). They also showed the presence of “inflammatory cells in the interstitium in animals less than 6 months of age and alveolar macrophages. Furthermore they demonstrated that the entire proximal and distal airways were diffusely encrusted in a thick coating of mucus-like material at all ages, which completely enveloped the ciliated surface (36, 71). From 1 month of age, SEM of the surface of the bronchiolar epithelial cells of affected animals demonstrated that the cilia were embedded in this material, as were the alveolar walls. Morphometric determination of alveolar interstitial thickness demonstrated a significant age-related increase in the affected animals. Type II pneumocytes were flatter than their wild-type counterparts and many lacked normal looking lamellar bodies (36). These data suggest that the basic defect in CF is also expressed in the periphery of the airways, i.e., the alveoli. Indeed, CFTR is expressed in rat lung alveoli in type II pneumocytes (72). Also results from our laboratory (M. Ulrich, unpublished) reveal the presence of CFTR in normal human lung tissue in type II pneumocytes. However, in the present study, neither NKT cells nor macrophages or neutrophils were significantly increased in alveolar sections of mouse lungs in comparison to the respective wild type tissues (data not shown). Similarly, accumulation of cells of the innate immune system was not significantly different from control mice in the bronchial epithelium, where CFTR is thought to be present in ciliated cells (15). Thus, one can conclude that the observed accumulation of cells of the innate immune system in the present study is restricted to areas of highest CFTR expression, i.e., the submucosal glands (14).

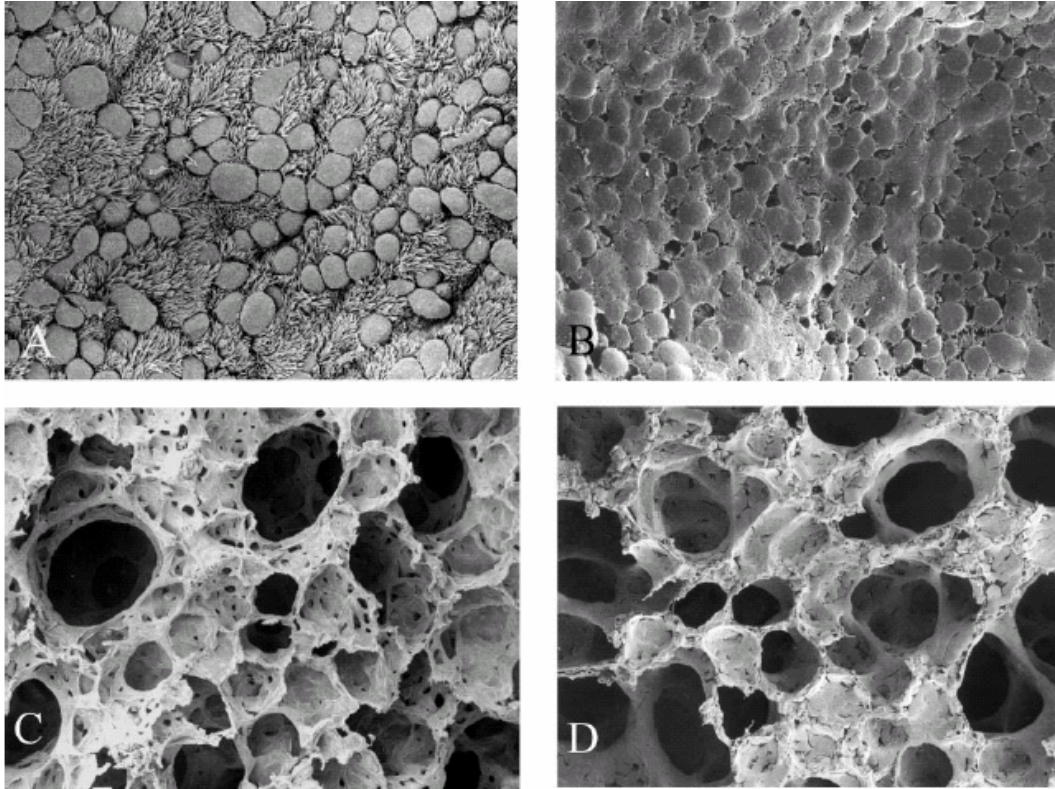


**Fig. 26. A:** SEM of the surface of the respiratory epithelium from a terminal bronchiole in an 11-month-old wild-type animal. Note the numerous ciliated and nonciliated cells. **B:** Terminal bronchiole from a *Cfr*<sup>-/-</sup> littermate. Respiratory epithelium is encrusted in mucus-like material. **C:** Alveoli from the wild-type animal. **D:** Alveoli from the affected animal. Distal airways were caked with mucus-like material. Original magnifications: x1000 (A, B); x650 (C, D) (from [36]).

Whether the results which were obtained in CF mouse strains are also present in human CF patients is unclear at present. Clearly, early bacterial lung infection in CF patients confounds the picture of the immune response, observed in non-infected CF mice. An alternative is to investigate human fetal lung tissue. In lungs of human CF fetuses the number of alveolar macrophages increased during fetal development in contrast to macrophage numbers in human non-CF lungs (CF,  $106 \pm 8.0$  cells/mm<sup>2</sup>; non-CF,  $17 \pm 11.1$  cells/mm<sup>2</sup>;  $P < .001$ ) (**Fig. 27**) (20). The authors hypothesized that alveolar macrophages play a prominent role for in the early onset of pulmonary disease in patients with CF, however, they admit that the nature of dysregulated signals in the local immunity generated by the CF fetal airways remains to be elucidated. They also showed that the epithelial differentiation and maturation in CF tissues were similar to those in non-CF controls during fetal airway de-

velopment (20), corroborating similar observations in *cftr<sup>m1HGU</sup>/cftr<sup>m1HGU</sup>* mice (73). In lungs of human CF fetuses, the submucosal glands showed “normal secretions” without hypertrophy and the number and distribution of mucous cells were similar in CF and non-CF fetuses (20). The differences between these findings and the results of the present study may relate to the notion that submucosal glands (and CFTR) function differently before and after birth. Thus, in further studies it may be interesting to determine the onset of NKT cell accumulation in younger mice than used in the present study including murine or human fetuses.

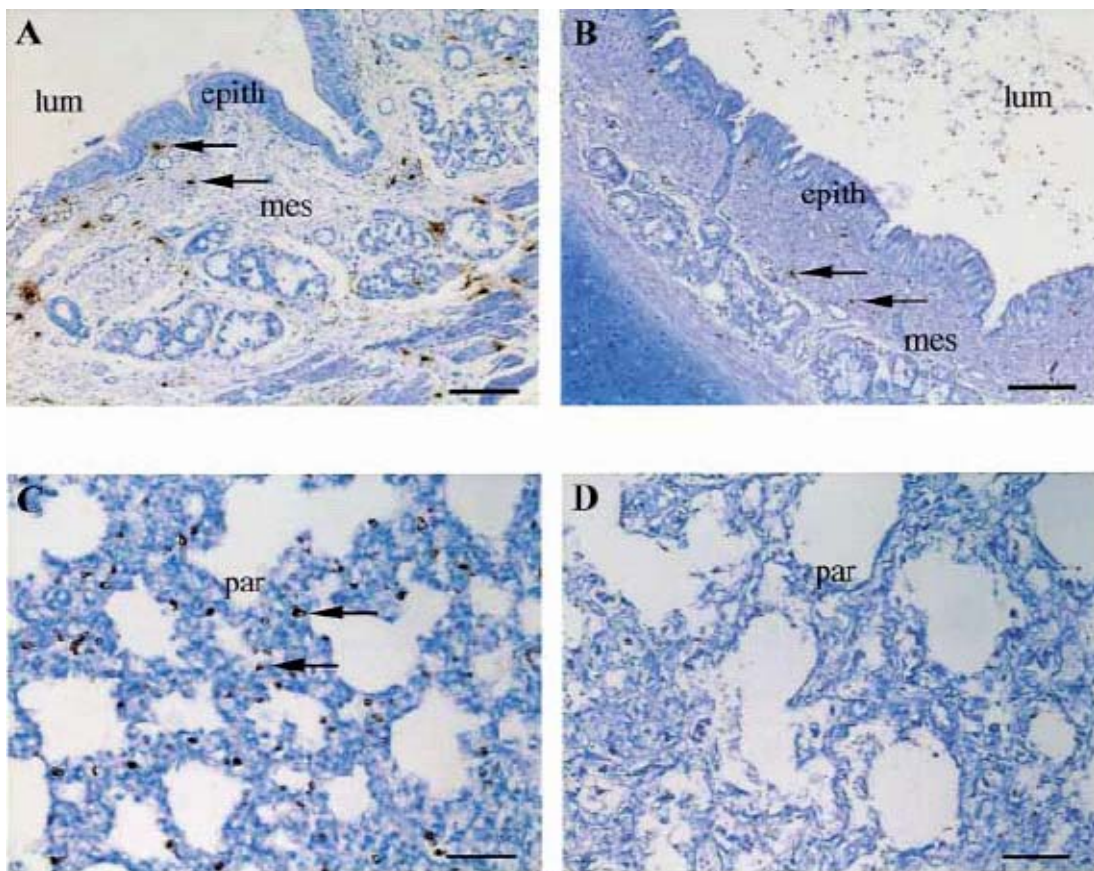


**Fig. 27.** Immunohistochemical detection of mast cells (trachea) and macrophages (lung) in CF and non-CF tissue sections. **A**, CF trachea at 36 weeks (**arrows** indicate mast cells). **B**, Non-CF trachea at 41 weeks. **C**, CF lung at 36 weeks (**arrows** indicate alveolar macrophages). **D**, Non-CF lung at 29 weeks. **lum**, Lumen; **epith**, surface epithelium; **mes**, mesenchyma; **par**, parenchyma. **Bars** represent 240  $\mu\text{m}$  (**A** and **B**) and 120  $\mu\text{m}$  (**C** and **D**) (from [20]).

Taken together, our data show that in CFTR<sup>-/-</sup> mice CD1d-restricted NKT cells accumulate in areas of CFTR expression in lungs and intestines. Additionally, ceramide expression is abnormally increased. Both ceramide and NKT cell accumulation increases with the age of the animals and provokes the accumulation of other cells of the innate and the adaptive immune system. This process can be normalized by blocking ASM which is responsible for the production of ceramide from sphingomyelin. Whether the inflammation provokes lung infection and other complications seen in the intestinal tract of CF patients is unclear at present.

## REFERENCES

1. Quinton PM. Physiological basis of cystic fibrosis: a historical perspective. *Physiol Rev* 1999; 79(1 Suppl):S3-S22.
2. Riordan JR, Rommens JM, Kerem BS, et al. Identification of the Cystic Fibrosis Gene: Cloning and characterization of complementary DNA. *Science* 1989; 245:1066-73.
3. Rommens JM, Iannuzzi MC, Kerem BS, et al. Identification of the Cystic Fibrosis Gene: Chromosome walking and jumping. *Science* 1989; 245:1059-65.
4. Kerem B-T, Rommens JM, Buchanan JA, et al. Identification of the cystic fibrosis gene: genetic analysis. *Science* 1989; 245:1073–1080.
5. The Cystic Fibrosis Genetic Analysis Consortium. Cystic Fibrosis Mutation Data Base. <http://www.genet.sickkids.on.ca/cftr/>
6. Vankeerberghen A, Cuppens H, Cassiman JJ. The cystic fibrosis transmembrane conductance regulator: an intriguing protein with pleiotropic functions. *J Cystic Fibrosis* 2002; 1:13–29.
7. Boucher RC, Stutts MJ, Knowles MR, Cantley L, Gatzky JT. Na<sup>+</sup> transport in cystic fibrosis respiratory epithelia. Abnormal basal rate and response to adenylate cyclase activation. *J Clin Invest* 1986; 78:1245-52.
8. Riordan JR. Assembly of functional CFTR chloride channels. *Annu Rev Physiol* 2005; 67:701-18.
9. Borst P, Elferik RO. Mammalian ABC transporters in health and disease. *Annu Rev Biochem* 2002; 71:537-92.
10. Lewis HA et al. Structure of nucleotide-binding domain 1 of the cystic fibrosis transmembrane conductance regulator. *EMBO J.* 2004; 23:282-93.
11. Kunzelmann K. Control of membrane transport by the cystic fibrosis transmembrane conductance regulator (CFTR). In: Kirk KL, Dawson DC, editors. *The cystic fibrosis transmembrane conductance regulator*. Georgetown, TX: Landes Bioscience p 55-93.
12. Bence NF, Sampat RM, Kopito RR. Impairment of the ubiquitin-proteasome system by protein aggregation. *Science* 2001; 292:1552-5.
13. Short DB, Trotter KW, Reczek D, et al. An apical PDZ protein anchors the cystic fibrosis transmembrane conductance regulator to the cytoskeleton. *J Biol Chem* 1998; 273:19797-801.

14. Engelhardt JF, Yankaskas JR, Ernst SA, et al. Submucosal glands are the predominant site of CFTR expression in the human bronchus. *Nature Genetics*. 1992; 2:240-8.
15. Kreda SM, Mall M, Mengos A, et al. Characterization of wild-type and deltaF508 cystic fibrosis transmembrane regulator in human respiratory epithelia. *Mol Biol Cell* 2005; 16:2154-67.
16. Mall M, Kreda SM, Mengos A, et al. The DeltaF508 mutation results in loss of CFTR function and mature protein in native human colon. *Gastroenterology* 2004; 126:32-41.
17. Ratjen F, Doring G. Cystic fibrosis. *Lancet* 2003; 361:681-9.
18. Lloyd-Still JD. Pulmonary manifestations, In: *Textbook of Cystic Fibrosis* Lloyd-Still JD, (ed) Boston: John Wright 1983: 165-198.
19. Jayaraman S, Joo NS, Reitz B, Wine JJ, Verkman AS. Submucosal gland secretions in airways from cystic fibrosis patients have normal [Na(+)] and pH but elevated viscosity. *Proc Natl Acad Scie USA* 2001; 98:8119-23.
20. Hubeau C, Puchelle E, Gaillard D. Distinct pattern of immune cell population in the lung of human fetuses with cystic fibrosis. *J. Allergy Clin Immunol* 2001; 108:524-49.
21. Abman SH, Ogle JW, Harbeck RJ, et al. Early bacteriologic, immunologic, and clinical courses of young infants with cystic fibrosis identified by neonatal screening. *J Pediatr* 1991; 119:211-7.
22. Khan TZ, Wagener JS, Bost T, et al. Early pulmonary inflammation in infants with cystic fibrosis. *Am J Respir Crit Care Med* 1995; 151:1075-82.
23. Niederman MS, Merrill WW, Polomski LM, et al. Influence of sputum IgA and elastase on tracheal cell bacterial adherence. *Am Rev Respir Dis* 1986; 133:255-60.
24. Plotkowski MC, Beck G, Tournier JM, et al. Adherence of *Pseudomonas aeruginosa* to respiratory epithelium and the effect of leucocyte elastase. *J Med Microbiol* 1989; 30:285-93.
25. Greene CM, Carroll TP, Smith SG, et al. TLR-induced inflammation in cystic fibrosis and non-cystic fibrosis airway epithelial cells. *J Immunol* 2005; 174:1638-46.
26. Weber AJ, Soong G, Bryan R, et al. Activation of NF-kappaB in airway epithelial cells is dependent on CFTR trafficking and Cl<sup>-</sup> channel function. *Am J Physiol Lung Cell Mol Physiol* 2001; 281:L71-8.
27. Joseph T, Look D, Ferkol T. NF-kappaB activation and sustained IL-8 gene expression in primary cultures of cystic fibrosis airway epithelial cells stimulated with Pseu-



- Pseudomonas aeruginosa*. Am J Physiol, 2005; 288:L471-L479.
28. Hubeau C, Lorenzato M, Couetil JP, et al. Quantitative analysis of inflammatory cells infiltrating the cystic fibrosis airway mucosa. Clin Exp Immunol, 2001; 124:69-76.
  29. Dorin JR, Dickinson P, Alton EW, Smith SN, Geddes DM, Stevenson BJ, Kimber WL, Fleming S, Clarke AR, Hooper ML. Cystic fibrosis in the mouse by targeted insertional mutagenesis. Nature 1992; 359:211-5.
  30. Zhou L, Dey CR, Wert SE, DuVall MD, Frizzell RA, Whitsett JA. Correction of lethal intestinal defect in a mouse model of cystic fibrosis by human CFTR. Science 1994; 266:1705-8.
  31. Delaney SJ, Alton EW, Smith SN, Lunn DP, Farley R, Lovelock PK, Thomson SA, Hume DA, Lamb D, Porteous DJ, Dorin JR, Wainwright BJ. Cystic fibrosis mice carrying the missense mutation G551D replicate human genotype-phenotype correlations. EMBO J 1996; 15:955-63.
  32. Zahm JM, Gaillard D, Dupuit F, et al. Early alterations in airway mucociliary clearance and inflammation of the lamina propria in CF mice. Am J Physiol 1997; 272:C853-C859.
  33. Tirouvanziam R, de Bentzmann S, Hubeau C, et al. Inflammation and infection in naive human cystic fibrosis airway grafts. Am J Respir Cell Mol Biol, 2000; 23:121-7.
  34. Tirouvanziam R, Khazaal I, Peault B. Primary inflammation in human cystic fibrosis small airways. Am J Physiol 2002; 283:L445-51.
  35. Du M, Jones JR, Lanier J, et al. Aminoglycoside suppression of a premature stop mutation in a *Cftr*<sup>-/-</sup> mouse carrying a human CFTR-G542X transgene. J Mol Med 2002; 80:595-604.
  36. Durie PR, Kent G, Phillips MJ, et al. Characteristic multiorgan pathology of cystic fibrosis in a long-living cystic fibrosis transmembrane regulator knockout murine model. Am J Pathol 2004; 164:1481-93.
  37. Coleman FT, Mueschenborn S, Meluleni G, et al. Hypersusceptibility of cystic fibrosis mice to chronic *Pseudomonas aeruginosa* oropharyngeal colonization and lung infection. Proc Natl Acad Sci 2003; 100:1949-54.
  38. van Heeckeren AM, Schluchter MD, Drumm ML, Davis PB. Role of *Cftr* genotype in the response to chronic *Pseudomonas aeruginosa* lung infection in mice. Am J Physiol 2004; 287:L944-L952.
  39. Mall M, Grubb BR, Harkema JR, et al. Increased airway epithelial Na<sup>+</sup> absorption produces cystic fibrosis-like lung disease in mice. Nat Med 2004; 10: 487-93.



40. Armstrong DS, Grimwood K, Carlin JB, et al. Lower airway inflammation in infants and young children with cystic fibrosis. *Am J Respir Crit Care Med* 1997; 156:1197-1204.
41. Armstrong DS, Hook SM, Jansen KM, et al. Lower airway inflammation in infants with cystic fibrosis detected by newborn screening. *Pediatr Pulmonol* 2005; 40:500-10.
42. Krivan HC, Roberts DD, Ginsburg V. Many pulmonary pathogenic bacteria bind specifically to the carbohydrate sequence GalNAc $\beta$ 1-4Gal found in some glycolipids. *Proc Natl Acad Sci USA* 1988; 85:6157-61.
43. Imundo L, Barasch J, Prince A, Al-Awqati Q. Cystic fibrosis epithelial cells have a receptor for pathogenic bacteria on their apical surface. *Proc Natl Acad Sci USA* 1995; 92:3019-23.
44. Ulrich M, Herbert S, Berger J, et al. Localization of *Staphylococcus aureus* in infected airways of patients with cystic fibrosis and in a cell culture model of *S. aureus* adherence. *Am J Respir Crit Care Med* 1998; 18:1.
45. Worlitzsch D, Tarran R, Ulrich M, et al. Effects of reduced mucus oxygen concentration in airway *Pseudomonas* infections of cystic fibrosis patients. *J Clin Invest* 2002; 109:317-25.
46. Pier GB, Grout M, Zaidi TS, et al. Role of mutant CFTR in hypersusceptibility of cystic fibrosis patients to lung infections. *Science* 1996; 271:64-7.
47. Smith JJ, Travis SM, Greenberg EP, Welsh MJ. Cystic fibrosis airway epithelia fail to kill bacteria because of abnormal airway surface fluid. *Cell* 1996; 85:229-36.
48. Boucher RC. New concepts of the pathogenesis of cystic fibrosis lung disease. *Eur Respir J* 2004; 23:146-58.
49. Matsui H, Grubb BR, Tarran R, et al. Evidence for periciliary liquid layer depletion, not abnormal ion composition, in the pathogenesis of cystic fibrosis airways disease. *Cell* 1998; 95:1005-.
50. Joo NS, Lee DJ, Wings KM, et al. Regulation of antiprotease and antimicrobial protein secretion by airway submucosal gland serous cells. *J Biol Chem* 2004; 279:38854-60.
51. Matsui H, Verghese MW, Kesimer M, et al. Reduced three-dimensional motility in dehydrated airway mucus prevents neutrophil capture and killing bacteria on airway epithelial surfaces. *J Immunol* 2005; 175:1090-9.
52. Bendelac, A., M. N. Rivera, S. H. Park, and J. H. Roark. Mouse CD1-specific NK1 T cells: development, specificity, and function. *Annu. Rev. Immunol* 1997; 15:535-62.

53. Kronenburg M, Gapin L. The unconventional life style of NKT cells. *Nat Rev Immunol* 2002; 2:557-68.
54. Zajonc DM, Cantu C 3rd, Mattner J, Zhou D, Savage PB, Bendelac A, Wilson IA, Teyton L. Structure and function of a potent agonist for the semi-invariant natural killer T cell receptor. *Nature Immunol* 2005; 6:810-8.
55. Apostolou I, Takahama Y, Belmant C, Kawano T, Huerre M, Marchal G, Cui J, Taniguchi M, Nakauchi H, Fournie JJ, Kourilsky P, Gachelin G. Murine natural killer cells contribute to the granulomatous reaction caused by mycobacterial cell walls. *Proc Natl Acad Sci USA* 1999; 96:5141-6.
56. Zhou D, et al. Lysosomal glycosphingolipid recognition by NKT cells. *Science* 2004; 306:1786-9.
57. Mattner J et al. Exogenous and endogenous glycolipid antigens activate NKT cells during microbial infection. *Nature* 2005; 434:525-9.
58. De Libero G, Mori L. Recognition of lipid antigens by T cells. *Nature Rev Immunol* 2005; 5:485-96.
59. Godfrey DI, Pellicci DG, Smyth MJ. The elusive NKT cell antigen – is the search over? *Science* 2004; 306:1687-8.
60. Godfrey DI et al. *Nat Rev Immunol* 2004;4: 231
61. Taniguchi M. The regulatory role of V $\alpha$ 14 NKT cells in innate and acquired immune response. *Annu Rev Immunol* 2003. 21:483-513.
62. Hannun YA, Obeid LM. The Ceramide-centric universe of lipid-mediated cell regulation: stress encounters of the lipid kind. *J Biol Chem* 2002; 277:25847-50.
63. Petrache I, Natarajan V, Zhen L, Medler TR, Richter AT, Cho C, Hubbard WC, Berdyshev EV, Tudor RM. Ceramide upregulation causes pulmonary cell apoptosis and emphysema-like disease in mice. *Nature Med* 2005; 11:491-8.
64. Cheng PW, Boat TF, Cranfill K, Yankaskas JR, Boucher RC. Increased sulfation of glycoconjugates by cultured nasal epithelial cells from patients with cystic fibrosis. *J Clin Invest* 1989; 84:68-72.
65. Rhim AD, Stoykova LI, Trindade AJ, Glick MC, Scanlin TF. Altered terminal glycosylation and the pathophysiology of CF lung disease. *J Cystic Fibrosis*. 2004; 3 (suppl 2):95-96.
66. Zhang Y, Doranz B, Yankaskas JR, Engelhardt JF. Genotypic analysis of respiratory mucous sulfation defects in cystic fibrosis. *J Clin Invest* 1995; 96:2997-3004.

67. Barasch J, al-Awqati Q. Defective acidification of the biosynthetic pathway in cystic fibrosis. *J Cell Science* 1993; 17:229-33.
68. Seksek O, Biwersi J, Verkman AS. Evidence against defective trans-Golgi acidification in cystic fibrosis. *J Biol Chem* 1996; 271:15542-8.
69. Poschet JF, Boucher JC, Tattersson L, Skidmore J, Van Dyke RW, Deretic V. Molecular basis for defective glycosylation and *Pseudomonas* pathogenesis in cystic fibrosis lung. *Proc Natl Acad Sci USA* 2001; 98:13972-7.
70. Kent G, Iles R, Bear CE, Huan LJ, Griesenbach U, McKerlie C, Frndova H, Ackerley C, Gosselin D, Radzioch D, O'Brodovich H, Tsui LC, Buchwald M, Tanswell AK: Lung disease in mice with cystic fibrosis. *J Clin Invest* 1997, 100:3060-9.
71. Kent G, Oliver M, Foskett JK, Frndova H, Durie P, Forstner J, Forstner GG, Riordan JR, Percy D, Buchwald M: Phenotypic abnormalities in long-term surviving cystic fibrosis mice. *Pediatr Res* 1996, 40:233-41.
72. Brochiero E, Dagenais E, Privé A, Berthiaume Y, Grygorczyk R. Evidence of a functional CFTR Cl<sub>-</sub> channel in adult alveolar epithelial cells. *Am J Physiol Lung Cell Mol Physiol* 2004; 287: L382-L392.
73. Geiser M, Zimmermann B, Baumann M. Does lack of *cftr* gene lead to developmental abnormalities in the lung? *Exp Lung Res* 2000; 26:551-64.

## 5. ABSTRACT

In cystic fibrosis (CF) dysfunction of CFTR leads to pathologic changes in several organs including lungs and intestine. Based on the notion that inflammation may precede infection in CF, the aim of this study was to investigate whether the CF defect would be recognized by cells of the innate immune system. Uninfected CF mouse strains and the respective wild type (WT) strains of different ages were used to locate and quantify NKT cells, macrophages and neutrophils and other immunocompetent cells in lung and intestine tissues. Furthermore the hypothesis was tested that ceramide accumulates in CFTR<sup>-/-</sup> cells. A significant increase in NKT cell numbers was observed in lung tissues of 12 week old CFTR<sup>-/-</sup> mice compared to WT mice. Mucin staining revealed that NKT cells accumulated around submucosal glands, known to express CFTR. NKT cell numbers further increased in 28 week old CFTR<sup>-/-</sup> mice around submucosal glands and in other parts of the lung including the alveolar septa, suggesting that the CF defect triggers a progressive innate immune response. Besides NKT cells, an accumulation of macrophages and neutrophils and other immunocompetent cells was observed around submucosal glands forming lymphocyte aggregates. In lung tissues of CFTR<sup>-/-</sup> mice, significantly increased concentrations of ceramide compared to control tissues were expressed in the area of submucosal glands and in other parts of the lung, including epithelial cells. The results suggest that defective CFTR provokes a high expression of ceramide which may lead to recognition by NKT cells possibly via endogenous glycosphingolipids. Treatment of CFTR<sup>-/-</sup> mice with amitriptyline, a blocker of acid sphingomyelinase, normalized the expression of ceramide and inhibited the clustering of NKT cells and macrophages around submucosal glands. High NKT cell expression was also observed in the lamina propria of jejunum, ileum and colon of CFTR<sup>-/-</sup> mice but not in control mice, further suggesting that the observed NKT cell recruitment in CFTR<sup>-/-</sup> mice is correlated to the basic CF defect. This data suggests that the basic defect in CF provokes an autoimmune response, characterized by ceramide over expression and early NKT cell accumulation around submucosal glands which thereafter is augmented and involved other effector cells of the innate immune system and immunocompetent cells of the adaptive immune system.

## **Curriculum vitae**

Name: Cheyla Conceicao de Oliveira-Munding  
Geburtsdatum/-ort: 08.12.1970, Angical/Bahia – Brasilien  
Familienstand: verheiratet, 1 Kind  
Eltern: Natalina Pereira de Souza,  
Ariosvaldo J. de Oliveira

### **Schulbildung:**

1978 - 1981 Grundschule (Aparício José da Silva) Bahia  
1982 - 1986 Gymnasium (Bom Jesus dos Milagres)  
1987 - 1990 Gymnasium (Centro Federal de Educação Tecnológica da Bahia)

### **Hochschulbildung:**

1990 -1995 Studium der Zahnmedizin an der Universidade Gama Filho, Rio de Janeiro (RJ), Brasilien  
13.01.1995 Zahnärztliche Prüfung  
1995 Aufbaustudium im Bereich Zahnprothese (acht Monate) an der UNIGRANRIO, RJ, Brasilien,

### **Praktische Studienzeiten:**

1993 Praktikum in Zahnstation Rocha Maia, RJ,  
Ambulanz für Odontopädiatrie, Endodontie, Chirurgie, Zahnfleischbehandlung  
1994 Pflichtpraktikum im Krankenhaus Notaufnahme, Rocha Faria, RJ  
Universitätspraktikum: Zahnklinik Marcolino Candau, RJ

### **Berufserfahrung:**

1995 - 1996 Klinik für allgemeine Zahnmedizin in São Cristovão, RJ  
1997 - 2002 Eigene Zahnarztpraxis für allgemeine Zahnmedizin in Salvador

## **Berufliche Weiterbildung:**

- 1996 Weiterbildungskurs: Dentistik und Zahnästhetik an der Universidade Federal Fluminense, Niteroi, RJ
- 1998 Teilnahme am X. Internationalen Kongress für Odontologie in Bahia  
Teilnahme am VIII. Brasilianischen Seminar für Mundpflege, Salvador  
Teilnahme am Kurs für Mundpflege und Vorbeugung von Mundkrankheiten, Salvador/Bahia
- Sep. 2004 Beginn der Promotion an der Universität Tübingen (bei Prof. Dr. Döring)

## **Danksagung**

Besonders bedanken möchte ich mich bei meinem Sohn Jonas, meiner Mutter und meinem Mann Johannes, die mir während meiner Promotion in schwierigen Phasen Halt gegeben und mich unterstützt haben.

Die vorliegende Arbeit wurde am Institut für Medizinische Mikrobiologie und Hygiene des Universitätsklinikums Tübingen, Direktor: Prof. Dr. Ingo Autenrieth, im Fach Immunologie durchgeführt.

Für das Überlassen des Themas und die freundliche und geduldige Betreuung während der Arbeit danke ich Herrn Prof. Dr. Gerd Döring.

Den Mitarbeitern des Hygieneinstitutes, die mich bei der Durchführung der Arbeit fachlich und menschlich unterstützt haben, insbesondere Dr. Martina Ulrich für die Betreuung, sowie Frau Gudrun Herer vom Mikrobiologischen Institut.

Für die Überlassung des Untersuchungsmaterials danke ich Herrn Prof. Dr. Erich Gulbins, Herrn Prof. Dr. Hugo de Jonge, Frau Dr. Anna Van Heckeren und Frau Dr. Uta Griesenbach.

Für die Unterstützung im histologischen Fragen möchte ich mich herzlichst bei Frau Prof. Dr. Marion Hewicker-Trautwein bedanken.